PHENOTYPIC AND COMPARATIVE ANALYSIS OF QUORUM SENSING MUTANTS IN *VIBRIO PARAHAEMOLYTICUS*

by

Jisoo Hong

A thesis submitted to the Faculty of the University of Delaware in partial fulfillment of the requirements for the degree of Bachelor of Arts in Biological Sciences with Distinction

Spring 2020

PHENOTYPIC AND COMPARATIVE ANALYSIS OF

QUORUM SENSING MUTANTS IN

VIBRIO PARAHAEMOLYTICUS

by

Jisoo Hong

Approved: _____

E. Fidelma Boyd, Ph.D.
Professor in charge of thesis on behalf of the Advisory Committee

Approved: _____

William Cain, Ph.D.
Committee member from the Department of Biological Sciences

Approved: _____

Gary H. Laverty, Ph.D.
Committee member from the Board of Senior Thesis Readers

Approved: _____

Michael Chajes, Ph.D.
Chair of the University Committee on Student and Faculty Honors

ACKNOWLEDGMENTS

The completion of this study would have been impossible without the overwhelming support and advice of many people. First, I express my sincere appreciation to my research advisor, Professor Boyd who has allowed and given me the opportunity to join her lab. Dr. Boyd has always been fully supportive and encouraging throughout my research journey at the University of Delaware, which has been an invaluable academic experience. This will remain with me as I progress from college. I would also like to thank my committee members, Dr. Cain and Dr. Laverty for their valuable and insightful comments.

When I first came into the lab, I was new to the world of scientific research. I wish to express my deepest gratitude to my graduate student mentor, Jessica Tague, who has invested a significant amount of time mentoring me through the entire research process. She has taught me methods, patiently guided me through critical thinking and analysis, and encouraged me to develop my abilities as a student researcher. I would also like to extend my appreciation to the remaining members of the Boyd Lab: Gwendolyn Gregory, Ji Kent Kwah, Katherine Boas, John Rosenberg, and Chun-kit Shum for all their support and insightful advice. Lastly, a great gratitude to my family and all my friends who have always been supportive, generous, and encouraging.

TABLE OF CONTENTS

LIST OF TABLES

LIST OF FIGURES

ABSTRACT

Quorum sensing is a type of bacterial cell-to-cell communication process using extracellular signaling molecules called autoinducers that reflect cell density. Bacteria respond to these autoinducers to detect changes in cell population and therefore alter gene expression. *Vibrio parahaemolyticus* is an enteric pathogen that causes gastroenteritis when consumed through raw or undercooked shellfish. We used *V. parahaemolyticus* as our model organism to study the quorum sensing pathway. In the *V. parahaemolyticus* quorum sensing pathway, at low cell density, quorum sensing response regulator LuxO is phosphorylated and activates sigma factor 54, also known as RpoN. Activated RpoN recruits RNA polymerase to initiate transcription of the five small quorum regulatory RNAs (*qrr1-qrr5*). The Qrr sRNAs post-transcriptionally stabilize *aphA* and degrade *opaR* mRNA transcripts. OpaR is the quorum sensing high cell density master regulator that has previously been shown to positively regulate the virulence factor capsule polysaccharide (CPS).

We investigated the role of the Qrr sRNAs in CPS production, swimming, and swarming motility. We examined six strains: wild type, Δ*opaR*, Δ*qrr* null (no *qrr*s), Δ*qrr1,3,4,5*, Δ*qrr1,2,3,5* and Δ*qrr1,2,3,4,* and determined that the Δ*qrr1,3,4,*5 mutant restored the expression of wild type CPS, swimming and swarming. This indicates that *qrr2* alone is capable of controlling the quorum sensing response in *V. parahaemolyticus*

Chapter 1

INTRODUCTION

1.1 Introduction to *Vibrio*

Members of the family *Vibrionaceae* are rod-shaped, gram-negative motile bacteria that are highly abundant in aquatic environments. *Vibrio* species inhabit estuaries and marine-coastal regions worldwide, and are a global concern of foodborne illness (46). By 2013, a total of 142 *Vibrio* species in the *Vibrio* genus have been identified (45). Of those species, the common *Vibrio* members associated with gastroenteritis pandemics are *Vibrio cholerae*, *Vibrio parahaemolyticus* and *Vibrio vulnificus* (54, 62). The infection cases in most *Vibrios* are caused by consuming contaminated water, undercooked fish and mollusks or through contact of an open wounds with contaminated seawater (6).

The occurrence of pathogenic *Vibrio* in the aquatic environments is highly dependent on the water temperature. A study has reported *Vibrio* population increased sharply as the water temperature rose from 10° to 20°C (5). Centers for Disease Control and Prevention (CDC) has estimated that each year in the United States, 80,000 illnesses and 100 deaths are caused by *Vibrio* species. Because *Vibrio* species

are highly abundant in warmer seawater, infections commonly occur between May and October (67).

1.2 Introduction to *Vibrio parahaemolyticus*

Vibrio parahaemolyticus is a halophilic bacterium and is the leading causes of the seafood-borne bacterial gastroenteritis worldwide. *Vibrio parahaemolyticus* naturally inhabits aquatic environments and are well distributed among shellfish such as oysters (9). Consumption of the raw seafoods that has been contaminated with the bacterium leads to the symptoms of diarrhea and nausea (52).

The outbreaks caused by *V. parahaemolyticus* have increased over two decades and incidents have been reported globally, commonly in Asian countries, Europe and the United States (52, 64). O3:K6 clinical serotype has been identified with reports of 345 *V. parahaemolyticus* infections between 1988 and 1997 (8). The first outbreak in the United States, was reported in 13 states by 416 people between May and July of 1998 (9). This case is one of the largest known gastroenteritis outbreaks due to this strain, found in Alaskan Oysters. This case suggests the rise of ocean water temperature could have contributed to the outbreak (32).

1.3 Quorum Sensing

Quorum sensing is a type of bacterial cell-to-cell communication process used by a wide range of bacterial populations. Bacteria produce membrane-diffusible molecules, called autoinducers, which can be secreted into the environment and

detected by other bacteria (37). The major class of autoinducers used by most gram-negative bacteria is N-acylated L-homoserine lactone molecules (AHLs) (7, 16, 34). The autoinducers are accumulated in the environment and act as ligands that bind to outer membrane receptors. As a result, the signal transduction pathway is triggered. Using these intracellular chemical signals, bacteria monitor population density and display group behaviors by altering their gene expression (34). It is known that at low cell density (LCD), organisms present asocial, individual behaviors while at high cell density (HCD) organisms present group and social behaviors (34).

In general, *Vibrio* species have been great model organisms in studying quorum sensing and its regulatory pathway. The bioluminescent organism, *Vibrio harveyi,* is an important model to study quorum sensing. The quorum sensing pathway components in *V. harveyi,* is conserved in our model organism *V. parahaemolyticus* (65). Thus, previous work from *V. harveyi* can be used as a guide to better understand the quorum sensing cascade of *V. parahaemolyticus*.

In a consensus quorum sensing cascade (Figure 1), at low cell density (LCD), the accumulated autoinducers in the environment are relatively low. A low concentration of ligands leads to a lack of receptor bindings, which results in the phosphorylation of the receptor kinases by ATP (34). The phosphate group from the phosphorylated receptor is then transferred to the phosphotransferase protein, LuxU (34, 65). P-LuxU phosphorylates the quorum sensing regulator LuxO which activates sigma factor 54 (σ^{54}), also known as RpoN (27). RpoN is unique amongst other sigma factors in that it has a -12 and-24 consensus binding site and requires activation for

transcription initiation (3, 33). LuxO and RpoN, along with RNA polymerase, initiate transcription of five small quorum regulatory RNAs, called *qrrs1-5* that stabilize *aphA* and degrade *opaR* mRNA transcripts. AphA is the master regulator of the low cell density quorum sensing pathway (57).

At high cell density, the phosphorelay cascade is the opposite of that at low cell density. High concentrations of autoinducers bind to the receptor proteins and no phosphorylation occurs. The inactivation of the phosphorylation circuit leads to the inactivation of LuxO. Unphosphorylated LuxO ultimately results in the lack of *qrrs* transcriptions and leads to the translation of the LuxR homolog, OpaR. OpaR is known as the high cell density master regulator (31, 34, 65). The master quorum sensing regulators play important roles in essential functions. These regulators are involved in the utilization of the carbon sources, colonization, production of the virulence factors amongst more (24, 63). For example, the HCD master regulator, OpaR, is a positive regulator of capsule polysaccharide (CPS) (19, 57).

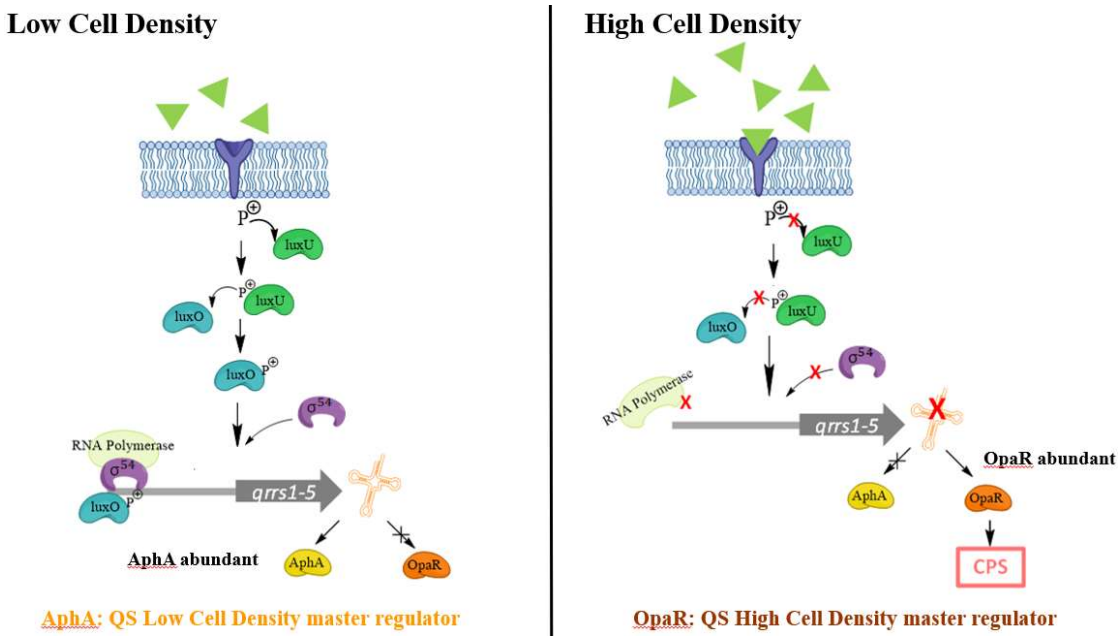

Figure 1 At LCD, the quorum sensing response regulator LuxO is phosphorylated and along with RpoN results in transcription of small quorum regulatory RNAs, called *qrrs1-5*. The Qrr sRNAs post-transcriptionally stabilize mRNA of *aphA,* the quorum sensing low cell density master regulator. At high cell density, LuxO is not phosphorylated and the inactivation of the phosphorylation cascade results in no transcription of Qrr sRNAs. This leads to the stabilization of *opaR* mRNA, the quorum sensing high cell density master regulator.

1.4 Small Quorum Regulatory RNAs (Qrrs) in *Vibrio*

Small RNAs (sRNAs) are non-coding molecules that regulate gene expression by inhibiting or activating target mRNAs. Qrr sRNAs are part of *trans*-encoded regulatory sRNAs present in a large number of bacteria (61). sRNA usually function through base pairing with and alteration of secondary structures in the 5′ untranslated regions (UTRs) of mRNAs (14). This base pairing at the ribosome-binding site can either induce translation or repress translation by occlusion of ribosomes (61). sRNAs

are 50 – 400 nucleotides long and undergo RNA-RNA base-pairing, RNA-DNA base-pairings, or protein binding. sRNAs interact with mRNA molecules by base-pairing with the 5' UTR or 3' UTR of mRNAs (36, 39, 61). More specifically, they generally base pair with the Shine-Dalgarno (SD) sequence, start codon or the coding sequences of the mRNA and occupy the ribosomal binding site (12).

sRNAs can either be cis-encoded or trans-encoded. Cis-encoded sRNAs are located on the same genetic locus as their target RNA and interact autonomously via complementation with their targets (36). Trans-encoded sRNAs are between 50-300 nucleotides long and are located at different loci than their targets (39). Trans-sRNAs show only partial complementation to their target mRNA, therefore, in general, the mechanism associated with trans-sRNA involves the chaperone protein, Hfq in order to strengthen their interaction with their targets (4, 58, 59). It is known that trans-sRNA can engage in cellular responses to environmental changes or even in the regulation of virulence in some of the pathogenic strains (30).

The quorum regulatory RNAs called the Qrrs sRNAs are trans-acting small RNAs. (4, 12, 50). The Qrrs can either positively or negatively regulate their target mRNAs to post-transcriptionally stabilize or destabilize their target transcripts (12). In positive regulation, the Qrrs base-pairs with the 5' UTR of the target mRNA, with the assistance of Hfq enhancing the interaction. Through this anti-antisense base pairing, the ribosome binding site (RBS) of the target mRNA is revealed, allowing for translation. In negative regulation, the Qrrs pairs with the 5' UTR of the target and blocks the ribosome binding site. This inhibits the translation of the target mRNA.

Mostly in this scenario, the ribonuclease E (RNase E) is recruited and degrades the destabilized mRNA (12, 14, 39).

The Qrrs number is conserved between *V. harveyi* and *V. parahaemolyticus*. Qrrs play a very important role in the quorum sensing pathway allowing for rapid alteration of gene expression (65). From a study of quorum sensing in *V. harveyi,* it was shown that all five Qrr molecules have a secondary structure with four stem loops and each stem loop has a unique function. The first stem loop (SL1) can base-pair with the mRNA, but the interaction is limited to specific complementary targets. However, this loop also protects the mRNA from degradation by RNase E. The second stem loop (SL2) has a critical function, as it carries out the core-interaction with most target transcripts, due to the conserved pairing sequences it contains. The third stem loop (SL3) aids in stability and supports in base pairing, while the fourth stem loop (SL4) acts as a rho-independent terminator which functions to stop transcription (47, 48).

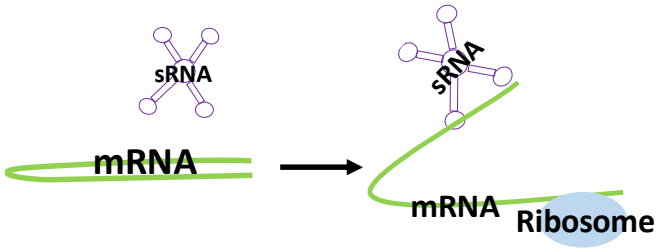

Figure 2 Schematic of the trans-encoded sRNA with the positive post-transcriptional regulation. The Hfq protein is not shown. The sRNAs partially complement with the target mRNA, carrying out the anti-antisense base pairing mechanism. The ribosome binding site is revealed, and the translation of the transcript occurs.

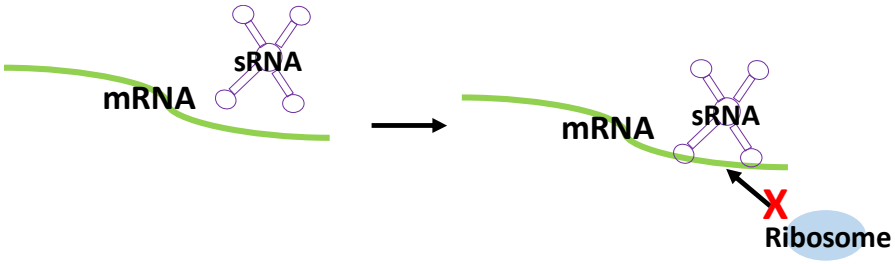

Figure 3 Schematic of the trans-encoded sRNA with the negative post-transcriptional regulation. The complementary pairings of sRNAs blocks the ribosome binding site of the target transcript. The mRNA is destabilized, and the translation does not occur.

1.5 *Vibrio parahaemolyticus* Capsule Polysaccharide

V. parahaemolyticus is a marine-estuarine enteric pathogen that has adapted to life on surfaces and the colonization in human intestines. In the canonical HCD quorum sensing pathway, Qrrs1-5 are down regulated, resulting in the stable *opaR* transcripts that produce OpaR, the positive regulator of CPS production (11, 19).

CPS also known as extracellular polysaccharide (EPS) creates a rough and opaque colony morphology. As the name 'polysaccharide' suggests, CPS materials consist of four major types of sugars: glucose, fucose, N-acetylglucosamine and galactose (11). This thick layer that surrounds the cell, presents the rugose colony phenotype.

CPS produced by *V. parahaemolyticus* is highly organized and therefore functions as a barrier against physical forces and abiotic stresses. Unlike opaque smooth translucent colonies, CPS production allows for structural integrity which

withstands stronger disturbances (11). The polysaccharide found in CPS also introduces sticky, adhesive characteristics, allowing for adherence to surfaces (22). As *V. parahaemolyticus* is an enteric pathogen, it is essential for cells to have the ability to adhere and colonize intestinal epithelial cells. CPS materials are also found to display an essential function in pellicle formation which produces a layer of protein film, or biofilm (19).

The *cpsA-K* operon has been identified as a locus encoding CPS biosynthesis (10). It is known that OpaR positively controls CPS production by indirectly regulating the CPS biosynthesis through two additional regulators (11, 15, 19). The OpaR deletion mutant does not form CPS and presents an opaque, smooth colony phenotype (31).

1.6 Motility of *Vibrio parahaemolyticus*: Swimming and Swarming

Movement is essential for bacteria to exhibit chemotaxis behaviors in response to the nutrient sources, chemical signals, threats, or group behaviors in an environment. Many bacterial species synthesize flagellum, a complex-structured appendage consisting of three parts: the filament, the basal structure, and the hook. Cells rotate these flagella to achieve various movement patterns, including swarming and swimming (53).

Vibrio parahaemolyticus is a great model organism in the study of motility due to its ability to both swim and swarm using polar and lateral flagella respectively. On a liquid surface, cells swim using a single, polar flagellum, however, when on a solid

surface, the bacterium transitions to swarmer cells using multiple lateral flagella. Using these peritrichous flagella, cells display collective swarming movements, which consumes the proton motive force (1, 25, 44, 49).

The quorum sensing regulators, AphA and OpaR have been examined in their regulation of swimming and swarming. The LCD master regulator, AphA activates swimming and swarming behaviors of the cell by regulating genes encoded for flagella biosynthesis (43, 60). The HCD master regulator, OpaR represses swarming, through upregulation of the second messenger c-di-GMP (13, 51, 55).

1.7 Aims of the Study

According to the canonical quorum sensing cascade, the small quorum regulatory RNAs (Qrrs) are involved in the translation of the LCD and inhibition of the HCD quorum sensing master regulators. The HCD master regulator, OpaR, is shown to positively regulate the production of capsule polysaccharide (CPS).

The overall goal of the study is to investigate the role of quorum sensing regulator mutants and their effects on three phenotypes of interest. We conducted phenotypic analysis of the mutant and performed computational comparative analysis of the *qrr* secondary structures. The three phenotypes of interest are CPS production, swimming, and swarming motility. To study the expression of these phenotypes in association with the Qrrs, a wild type *V. parahaemolyticus* and multiple quorum sensing mutant strains were used. The mutant strains used were Δ*opaR*, Δ*qrr* null (no *qrrs*), and mutants with only one *qrr* present. To accomplish this, we constructed three

mutants with a single *qrr* present by inserting via homologous recombination, *qrr1, qrr2 or qrr3* into the Δ*qrr* null mutant creating three quadruple *qrrs* mutants Δ*qrr2,3,4,5*, Δ*qrr1,3,4,5* and Δ*qrr1,2,4,5*.

To understand the regulatory role of each Qrr in *aphA* and *opaR* mRNA transcripts stability, we performed a computational analysis of predicted RNA-RNA interactions. In addition, the five *qrrs* coding regions were aligned to better understand the homology between them. Ultimately, we observed noteworthy stem loop pairing that perhaps suggest an individual role of each Qrr in the *V. parahaemolyticus* quorum sensing pathway.

Chapter 2

MATERIALS AND METHODS

2.1 Bioinformatics Analysis

An alignment of *Vibrio parahaemolyticus* small quorum regulatory RNAs (*qrrs*) *1-5* was created using the software T-Coffee (28, 35). To determine the interaction between the mRNAs of *opaR* and *aphA* with *qrrs1*-5, RNAhybrid Tool was used (26, 41). The results of the base-pairing regions obtained by the RNAhybrid software were located on the predicted structures of the Qrrs1-5. The structural folding of Qrrs1-5 was completed using the RNAfold WebServer software, ViennaRNA WebServices (66).

2.2 Bacterial Strains, Plasmids and Growth Conditions

All bacterial strains and plasmids were grown in aerobic conditions overnight at 37°C. Table 1 lists all the strains and plasmids used in the study. *Vibrio parahaemolyticus* strains were grown in Luria Bertani (LB) broth containing 3% NaCl. When required, the LB media was supplemented with 25µg/mL of chloramphenicol (Cm), 100µg/mL of ampicillin (Amp) or 10% sucrose. All *E. coli* strains were grown in LB media with 1% NaCl. *E. coli* β2155 *λpir* was grown in LB 1% NaCl, supplemented with 0.3mM of diaminopimelic acid (DAP), as it is a DAP auxotroph.

Table 1 All bacterial strains and plasmids used in the study

Strains and Plasmids	Genotype/Background
***Vibrio parahaemolyticus* (VP):**	
RIMD2210633	O3:K6 serotype
Δ*opaR*	RIMD2210633 with VP2516 deleted
Δ*qrr* null	RIMD2210633 with all wild type *qrrs1-5* deleted
Δ*qrr2,3,4,5*	RIMD2210633 Δ*qrr* null with wild type *qrr1* inserted
Δ*qrr1,3,4,5*	RIMD2210633 Δ*qrr* null with wild type *qrr2* inserted
Δ*qrr1,2,4,5*	RIMD2210633 Δ*qrr* null with wild type *qrr3* inserted
Δ*qrr1,2,3,5*	RIMD2210633 Δ*qrr* null with wild type *qrr4* inserted
Δ*qrr1,2,3,4*	RIMD2210633 Δ*qrr* null with wild type *qrr5* inserted
***Escherichia coli*:**	
β2155*λpir*	DAP auxotroph used in transformation and conjugation experiments
DH5*α*	Used in Transformation experiment and plasmid preparation
DH5*α* pDS132	DH5α containing pDS132 plasmid; Cm^R
Plasmids:	
pJET1.2	Cloning vector; Am^R
pJET1.2 wild type Vp *qrr2*	pJET1.2 vector containing wild type Vp *qrr2* insert
pDS132	Suicide vector with screening markers *SacB*, *pir*, *cat*; Cm^R
pDS132 wild type Vp *qrrs* (1/2/3)	pDS132 vector containing wild type Vp *qrr1*, pDS132 vector containing wild type Vp *qrr2* and pDS132 vector containing wild type Vp *qrr3*

2.3 Construction of *V. parahaemolyticus qrrs* Insertion Mutants

A summary of the constructed quadruple *qrrs* mutant strains which contain only one *qrr* are shown in Figure 4. The three quadruple *qrrs* mutants containing *qrr1*,

qrr2 or *qrr3* only were created through an insertion method. The amplified *qrr* fragment using primers A and D represents the wild type coding region of that corresponding gene. Each *qrr* AD fragment is inserted into the Δ*qrr* null mutant strain.

The remaining two *qrr* quad mutants were constructed using the deletion method in a wild type background. The Δ*qrr1,2,3,5* mutant, containing wild type *qrr4,* and the Δ*qrr1,2,3,4* mutant, containing wild type *qrr5,* were constructed previously using the deletion method in a wild type background. The aforementioned mutants were constructed while making the Δ*qrr* null mutant.

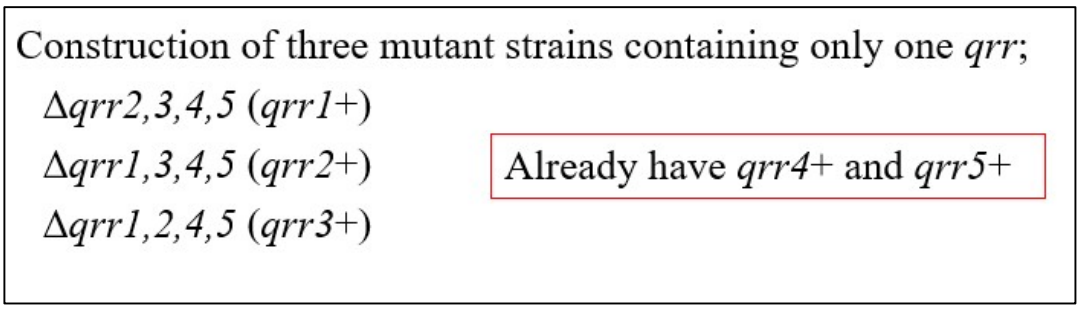

Figure 4 Overview of the constructed quadruple *qrrs* mutants containing *qrr1*, *qrr2* and *qrr3*. Each corresponding *qrr* was inserted into Δ*qrr* null mutant strain. Mutants containing *qrr4* and *qrr5* have been made previously thorough the deletion of *qrrs1,2,3,5* and *qrr1,2,3,4* respectively, in the wild type background.

2.3.1 Construction of pDS132 Vector with Wild Type *qrr1* Insert Product

A 1197 base-pair product of wild type *qrr1* AD fragment was amplified through High-fidelity Polymerase Chain Reaction (HF PCR) using previously designed Gibson Assembly primers. The fragment is digested with the restriction

enzyme SacI and assembled into pDS132 vector using Gibson Assembly protocol (17, 18).

2.3.2 Construction of pDS132 Vector with Wild Type *qrr2* Insert Product

Using *qrr2* AD primers, the 1068 base pairs of wild type *qrr2* AD insert was amplified through HF PCR (20, 21). Without the three extra base pairs at the 5'end of designed primers, the insert-fragment was cloned into pJET1.2 blunt end vector. The product was transformed in *E. coli* DH5α and spread on LB 1% NaCl agar plates, supplemented with Amp. Positive WT *qrr2* colonies that were selected through PCR screenings (Figure 6), were purified for digestion using restriction enzymes, SacI and XbaI. The purified DNA fragment containing single-stranded overhang regions was ligated into digested pDS132 vector.

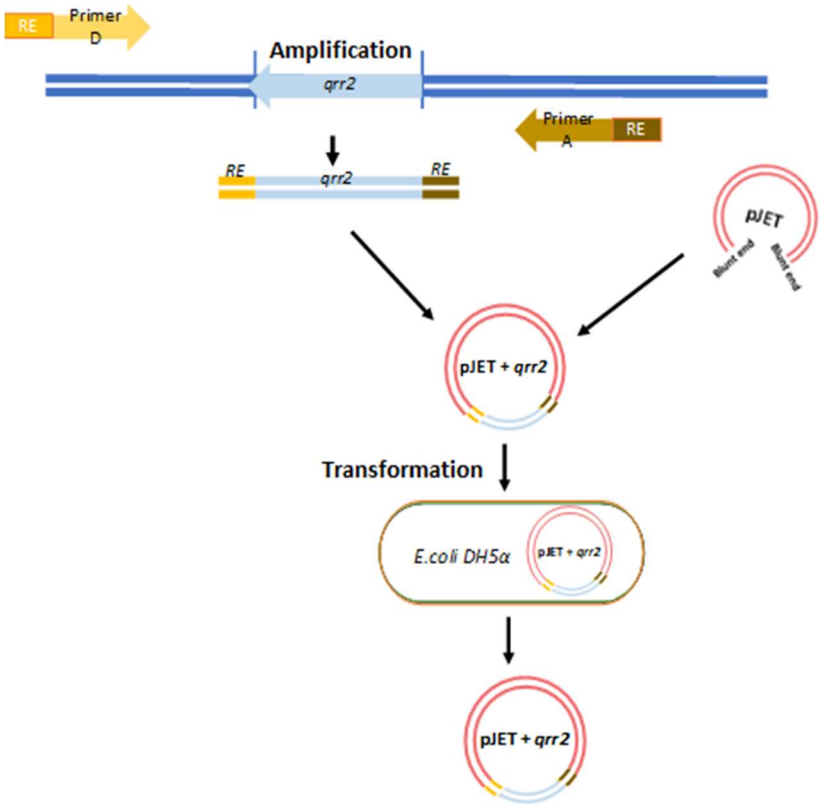

Figure 5 Workflow of wild type *qrr2*+pJET1.2 vector construction. Using the SOE *qrr2* AD primers, wild type *qrr2* was amplified from gDNA as a template. Wild type *qrr2* insert was ligated with the blunt end cloning vector, pJET1.2 and transformed to *E. coli* DH5*α* strain, on LB 1% NaCl with AMP plate.

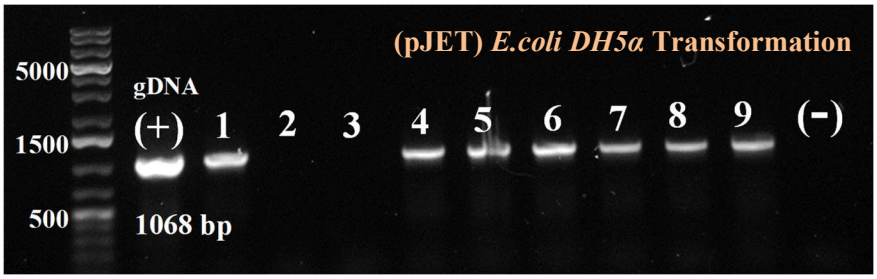

Figure 6 The PCR analysis of the constructed vector (pJET1.2 + wild type *qrr2*) using SOE *qrr2* AD primers and gDNA as positive control. The colonies (1,4-9) with the wild type *qrr2* size of 1068 bp are positives.

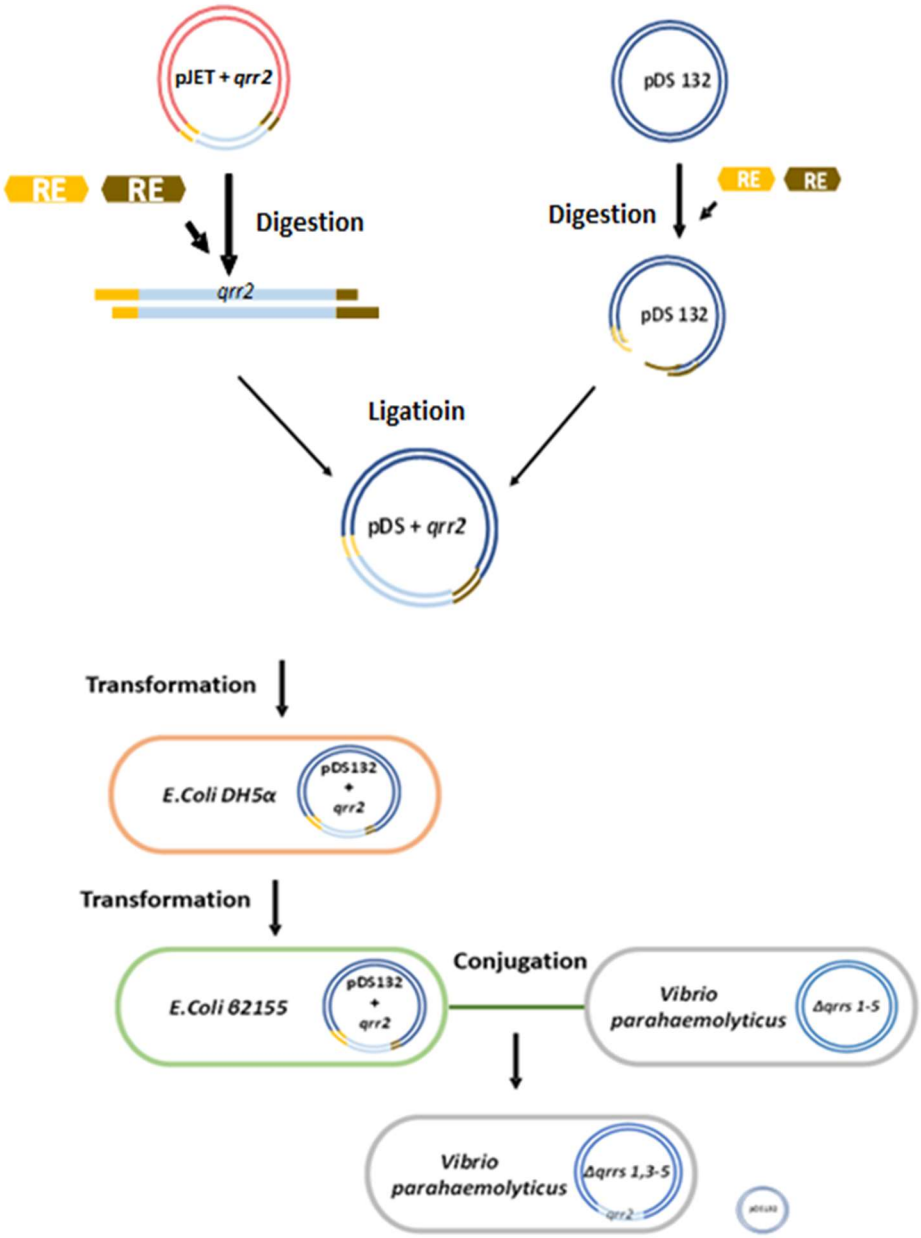

Figure 7 Continued schematic workflow of *qrr2* insertion mutant making process following the pJET1.2 cloning. Wild type *qrr2* is reinserted into Δ*qrr* null mutant via allelic exchange. Restriction enzymes SacI and XbaI were used for digestion of *qrr2* fragments and pDS132 plasmid. The product is transformed into to *E. coli* DH5*α*, purified, and transformed to *E. coli β2155λpir* that can be conjugated with *V. parahaemolyticus* Δ*qrr* null strain.

2.3.3 Construction of pDS132 Vector with Wild Type *qrr3* Insert Product

The SOE *qrr3* primers were used in HF PCR and amplified 1250 base pairs of wild type *qrr3* AD fragment. The primers were designed with three extra base pairs "CAC" at the 5'end in order to bypass the pJET1.2 cloning method. The *qrr3* insert-product was digested with PaeI and SacI and ligated with the cloning vector pDS132.

2.3.4 Bacterial Transformation

After the construction of pDS132 with each insert (Wild type *qrr1,* Wild type *qrr2* and Wild type *qrr3*), each vector containing the wild type coding region was transformed into *E. coli* DH5*α* competent cells (40) and 50mM of $CaCl_2$ were used during this process. Positively transformed colonies were selected using plates containing Cm and verified via PCR screenings. and the plasmids were purified (29). Plasmids from the positive colonies were harvested and transformed into *E. coli β2155λpir* using the same transformation protocol. The product of *E. coli β2155λpir* transformation was spread on LB 1% NaCl agar plates supplemented with Cm and 0.3 mM DAP. Positively screened colonies (shown in Figure 8), were incubated overnight for the conjugation procedure.

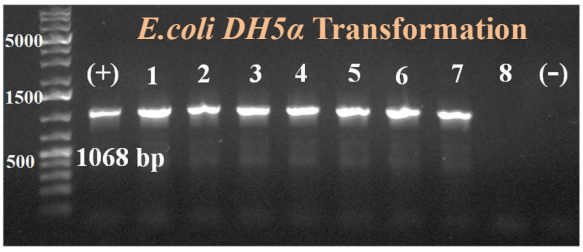

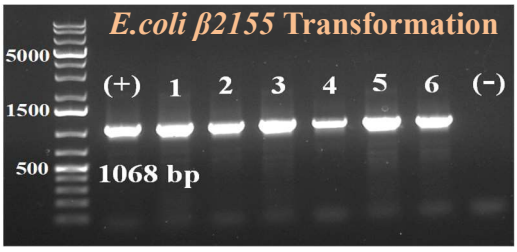

Figure 8 PCR analysis of vector pDS132 + wild type *qrr2* after each transformation. Each product of *E. coli* DH5α and *E. coli β2155λpir* transformations were spread plated onto LB1% NaCl Cm plates with DAP for *β2155λpir*. PCR screenings using the SOE *qrr2* AD primers ensured the correct product was transformed. gDNA is used as a positive control which yields 1068 bp of wild type *qrr2* bands.

2.3.5 Conjugation and Single Crossover Selection

E. coli β2155λpir + plasmid vector with each insert of interests was conjugated to the Δ*qrr* null strain on 1% NaCl LB agar plates, supplemented with 0.3mM DAP. After incubating the conjugation plate overnight, about one quarter of the lawn of cells was plated onto 3% NaCl LB agar plates containing Cm. As *V. parahaemolyticus* does not encode *pir* gene that is required for the replication of pDS132 (38), the plasmid is incorporated into the chromosome through single crossover (homologous recombination with AD product). Using colony PCR screenings with AD and flanking primers, colonies with the single crossover event were selected.

Figure 10 depicts confirmed positive colonies with the single crossover event. The gel in the left is the screening with *qrr2* AD primers and shows the wild type fragment size of 1068 bp. The gel in the left is the PCR reaction with *qrr2* flanking primers. The wild type *qrr2* flanking band is 1237 bp long and the wild type flanking bands are not shown in colonies with the single crossover event. The plasmid is incorporated into the genome and makes the fragment size too large to be amplified under the regular *qrr2* conditions.

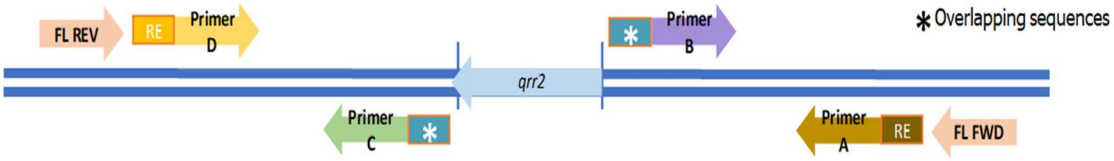

Figure 9 Schematic of the designed primers: SOE *qrr2* A, B, C, D, flanking forward and flanking reverse primers. Flanking primers were designed to amplify the extended section, including the AD regions.

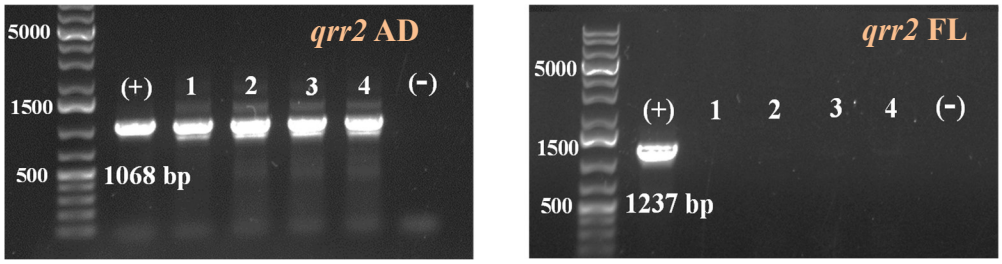

Figure 10 PCR analysis of the single crossover selection (pDS132+ wild type *qrr2* conjugation with *V. parahaemolyticus* Δ*qrr* null strain). Each colony served as PCR DNA templates for both SOE *qrr2* AD primers and Flanking primers. gDNA was used as positive controls for both PCR reactions. Successful single crossover colonies show wild type *qrr2* bands of 1068 bp and presents no flanking bands.

2.3.6 Plasmid Excision and Double Crossover Event

Positively selected single crossover colonies that were confirmed by PCR screenings were inoculated overnight in LB 3% NaCl without Cm. The absence of Cm in the plate initiates the loss of the plasmid incorporated in the genome. Serially diluted cultures were plated onto LB 3% NaCl agar plates with 10% sucrose. The pDS132 vector contains a cytotoxic *sacB* gene that is sensitive to sucrose (29, 38, 42).

As sucrose is toxic to pDS132, any healthy colonies that grew on the sucrose plates have excised the plasmid through the double crossover/homologous recombination with the AD product. Any unhealthy colonies appearing soupy or transparent on sucrose plates, indicating that the incorporated plasmid has not been lost from the chromosome. Healthy colonies were selected for PCR screenings with AD and flanking primers. Figure 11 shows healthy colonies (left panel) and soupy unhealthy colonies (right panel) of *qrr2* insertion mutant. Positive colonies contained *qrr1, qrr2* or *qrr3* product after allelic exchange during the double crossover events (Figure 12).

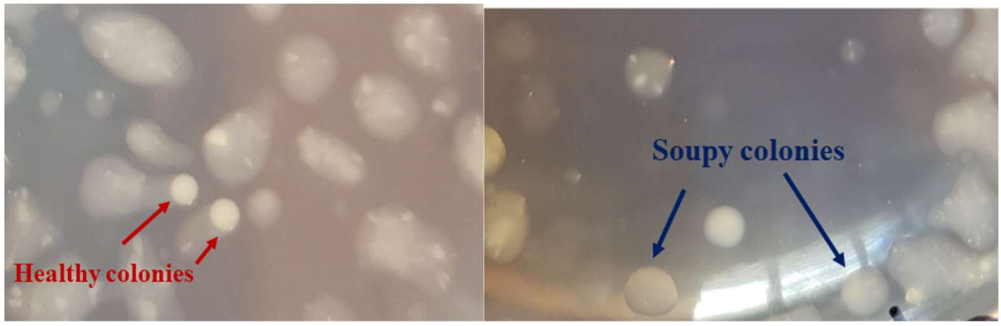

Figure 11 Double crossover colonies on LB 3% NaCl 10% sucrose plates. Left panel shows healthy colonies of wild type *qrr2* insertion mutant, which have successfully excised the plasmid, pDS132. Right panel presents unhealthy, soupy colonies of the wild type *qrr2* insertion mutant with transparent morphology. Only the healthy-looking colonies were selected for PCR screenings.

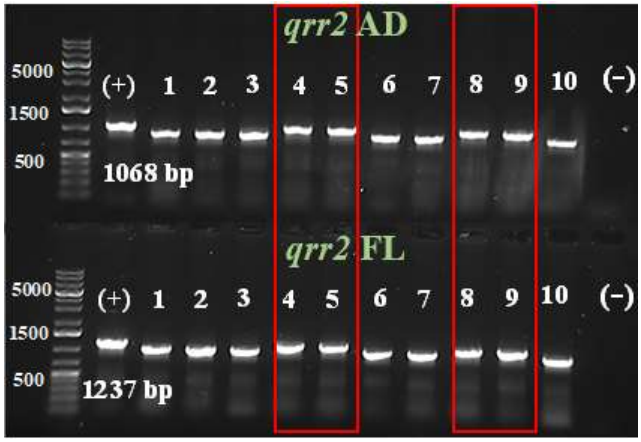

Figure 12 PCR analysis of the double crossover product (wild type *qrr2* insertion into *V. parahaemolyticus* Δ*qrr* null strain). Each of the healthy colony selected serve as templates for both SOE *qrr2* AD primers and Flanking primers. gDNA was used as positive controls for both PCR reactions. Successful double crossover colonies show 1068 bp of the wild type *qrr2* bands and 1237 bp of flanking bands as plasmids have been lost. The gel shows wild type *qrr2* remains inserted in colonies 4,5,8 and 9 out of 10 colonies.

2.4 Capsule Polysaccharide Assay

All strains of interests, including the wild type (WT) and Δ*opaR* used in this study (listed in Table 1) were inoculated on LB 3% NaCl agar plates the day before the assay. Fresh Capsule Polysaccharide (CPS) plates were prepared with Heart Infusion (HI) broth, 1.5% agar with 50 mg of Congo Red dye. 5 mL of 100mM $CaCl_2$ was added per 195mL dH_2O. Strains of interest were inoculated by touching the desired surface of CPS plates using a sterile pipette tip. Wild type RIMD2201633 was inoculated as a positive control and Δ*opaR* colonies was inoculated as a negative control. The plates are incubated at 30°C for 48 hours. Colonies characteristics were analyzed by comparing the phenotypes to that of the wild type.

2.5 Swimming Motility Assay

All strains used in the assay, including the positive control wild type RIMD2210633, were inoculated on LB 3% NaCl agar plates the day before. Semi-solid LB swimming plates were prepared with 0.3% of agar and 3% NaCl. Exactly 25 mL of the prepared swimming media was distributed to each plate and cooled for ten minutes. Only one strain per plate was stab-inoculated at the center using a sterile pipette tip. Swimming plates were incubated at 37°C for 18-24 hours as necessary. The assay was repeated in two biological replicates and each with three technical replicates. The diameters of the swimming colonies were measured, and data analyzed.

2.6 Swarming Motility Assay

The day before the assay, the wild type and strains of interest were inoculated on LB 3% NaCl agar plates. The solid LB swarming plates were prepared on the day of the assay, with 2% NaCl and 1.5% agar. The colonies were surface- inoculated using sterile pipette tips. The plates were incubated at 30°C for 48 hours before imaging.

Chapter 3

RESULTS

3.1 Confirmation of Δ*qrr1,3,4,5* mutant

After the double crossover event, *qrr2* insertion into the Δ*qrr* null was confirmed using PCR screenings with SOE *qrr2* AD and FL bands (Figure 12). To confirm the Δ*qrr1,3,4,5* mutant strain, screening with all *qrrs1-5* AD primers was performed. The agarose gel Figure 13 presents positive wild type *qrr2* bands showing the same band sizes as the positive control, which is the representation of the wild type *qrr2.* The coding regions of *qrr1*, *qrr3*, *qrr4* and *qrr5* have previously been deleted in the mutant strain, causing mutant sized bands compared to wild type length. Overall, Figure 13 confirms the Δ*qrr1,3,4,5* mutant by showing only *qrr2* has the wild type sized bands.

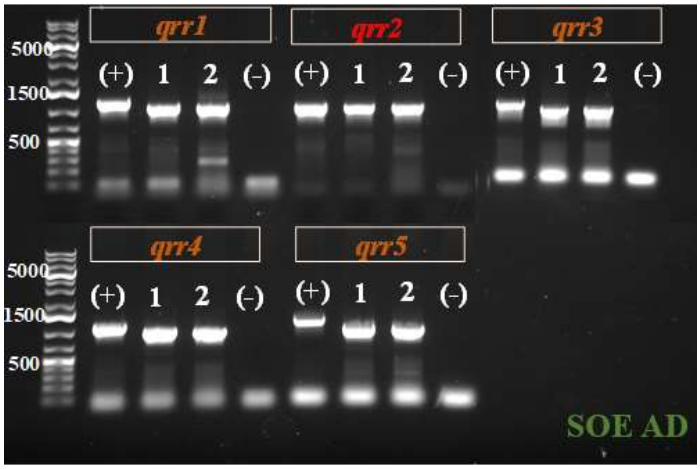

SOE AD primers

- *qrr1*: bands smaller than WT *qrr1* bands (+)
- ***qrr2***: WT *qrr2* bands
- *qrr3*: bands smaller than WT *qrr3* bands (+)
- *qrr4*: bands smaller than WT *qrr4* bands (+)
- *qrr5*: bands smaller than WT *qrr5* bands (+)

Figure 13 PCR analysis confirming the wild type *qrr2* insertion mutant. Two mutant colonies were selected and served as templates for all reactions with *qrrs1-5* AD primers. gDNA was used as positive controls for all reactions. All *qrrs* AD bands except *qrr2* present smaller band sizes when compared to the positive controls. The gel presents only wild type *qrr2* is inserted and *qrr1, qrr3, qrr4,* and *qrr5* are shown deleted.

3.2 *V. parahaemolyticus* Δ*qrr1,3,4,5* Restored the Wild Type CPS Phenotype

The expression of CPS in *V. parahaemolyticus* quorum sensing mutant strains was characterized and analyzed (Figure 14). Wild type was used as a positive control and Δ*opaR* was used a negative control. As *opaR* is known as a positive regulator of CPS expression, deletion of the gene leads to a smooth, translucent colony morphology (Figure 14). The other mutant strains used are Δ*qrr1,3,4,5*, Δ*qrr1,2,3,5*, Δ*qrr1,2,3,4* and Δ*qrr* null.

All tested *qrrs* mutant strains except Δ*qrr1,2,3,5* expressed various capsule polysaccharide phenotypes when compared to the negative control, Δ*opaR* (Figure 14). The Δ*qrr1,2,3,5* mutant did not produce CPS and presented a translucent, smooth colony morphology as appeared in Δ*opaR* (Figure 14). The Δ*qrr* null and Δ*qrr1,2,3,4* mutants had a very similar phenotype, but a very different colony morphology relative to wild type. These two colonies are smaller in size than the positive control but appeared to have a rough colony surface (Figure 14). We are currently unsure whether CPS is actually formed. The Δ*qrr1,3,4,5* mutant strain produced CPS and presented a wrinkled, rugose colony morphology very similar to wild type (Figure 14).

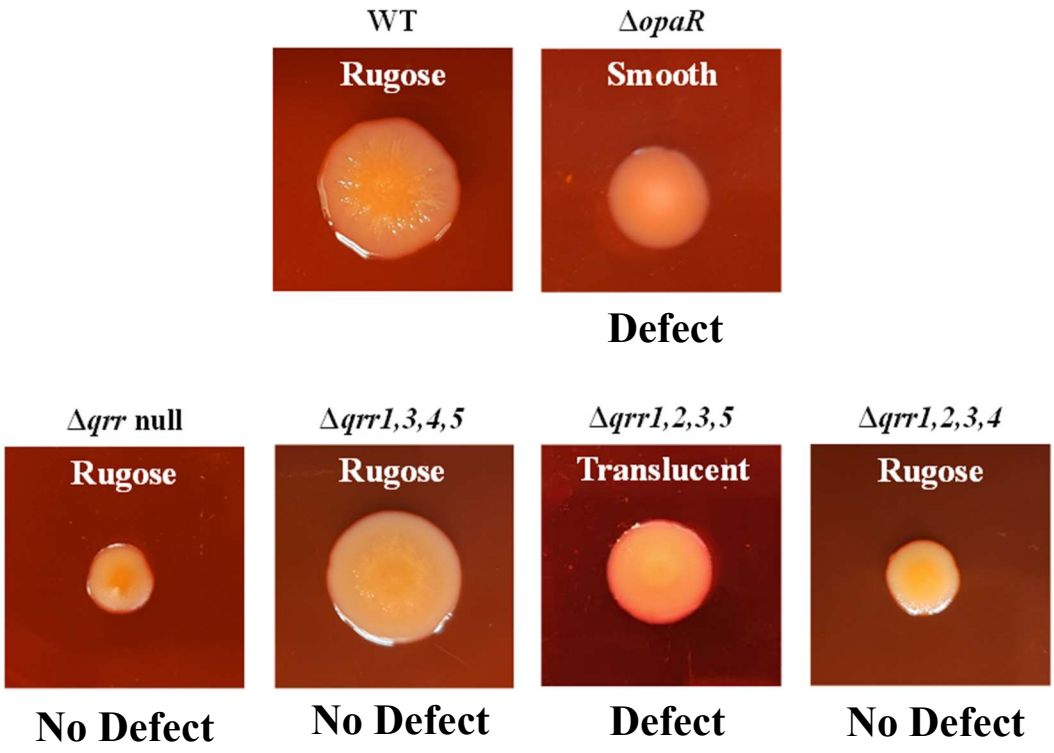

Figure 14 Capsule polysaccharide production as determined by colony morphology in the mutant strains. Wild type is used as a positive control and Δ*opaR* is used as a negative control with a translucent, non-CPS producing colony. The Δ*qrr1,2,3,5* mutant showed defect in CPS expression. The Δ*qrr* null and Δ*qrr1,2,3,4* mutants appeared in smaller colonies with rough surfaces, relative to wild type. The Δ*qrr1,3,4,5* mutant appeared to have restored the wild type CPS production.

3.3 *V. parahaemolyticus* Δ*qrr1,3,4,5* Restored Swimming Motility

The swimming motility of quorum sensing mutant strains were observed, indicating the use of a single, polar flagellum to swim in a semi-solid LB 3% NaCl media. Four strains used in the assay were wild type (WT) and mutants Δ*opaR*, Δ*qrr* null and Δ*qrr1,3,4,5*.

For the swimming assays, all strains were compared to the wild type positive control (Figure 15). The Δ*opaR* mutant is known as a hyper-swimmer and the swimming cells move across the plate (Figure 15). The Δ*qrr* null mutant presented less swimming motility than positive control (Figure 15). The Δ*qrr1,3,4,5* mutant also displayed swimming activity relative to wild type (Figure 15). The swimming assay results were quantified and are shown in Figure 16. The Δ*opaR* mutant showed a significantly higher average diameter relative to the wild type by p-value less than 0.01 (Figure 16). Oppositely, Δ*qrr* null showed a significantly lower mean value than the wild type by p-value less than 0.01 as well (Figure 16). However, statistics showed no significant difference between Δ*qrr1,3,4,5* swimming diameter from that of the wild type. Overall deletion of *qrrs1-5* caused a defect in swimming, while the presence of only *qrr2,* restored the wild type swimming behavior (Figure 16).

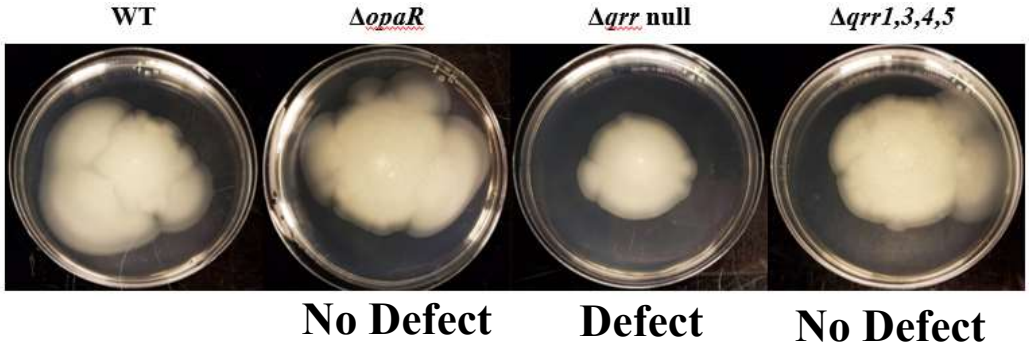

Figure 15 Swimming motility. Wild type was used as a positive control for the comparison with other tested strains. The Δ*opaR* mutant is known as a hyper-swimmer. The Δ*qrr* null mutant showed a lesser swimming motility when compared to the wild type. The Δ*qrr1*,*3,4,5* mutant was presented with a similar swimming phenotype as the wild type.

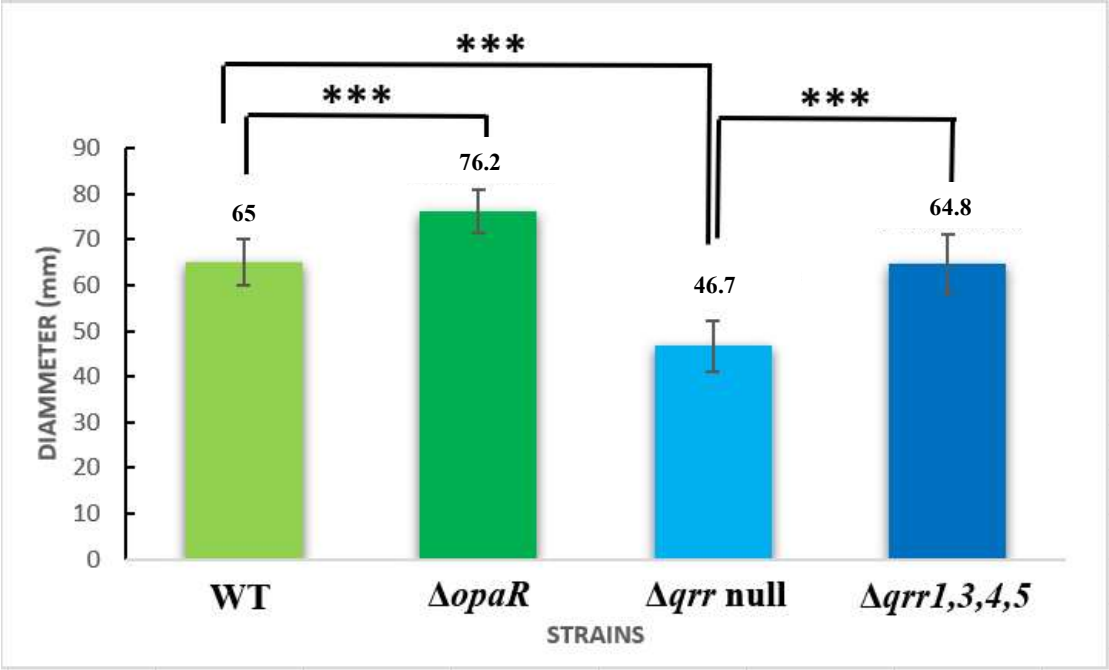

Figure 16 The average swimming diameters measured with the standard deviation. It is shown Δ*opaR* mutant has a significantly higher average of the swimming diameter compared to wild type. The Δ*qrr* null has a significantly lower average of the swimming diameter relative to wild type. The average diameter of Δ*qrr1,3,4,5* was shown to be significantly different from that of the Δ*qrr* null, but showed no significant differences compared to wild type. *** $p<0.01$

3.4 *V. parahaemolyticus* Δ*qrr1,3,4,5* Showed Wild Type Swarming Motility

The swarming assay was performed with six strains: wild type (WT), and Δ*opaR*, Δ*qrr1,3,4,5*, Δ*qrr1,2,3,5*, Δ*qrr1,2,3,4* and Δ*qrr* null mutants. These assays measure the present of lateral flagella that allow swarming behavior on a solid surface. All tested mutants were compared to wild type, the positive control (Figure 17). The Δ*opaR* mutant, known as a hyper swarmer, was also used as a control. As *opaR* is

known to repress the swarming behavior (23), thus deletion of the gene leads to the hyper swarming activity (Figure 17).

The assay results show Δ*qrr* null, Δ*qrr1,2,3,5* and Δ*qrr1,2,3,4* mutants had a defect in swarming motility (Figure 17). When compared to the positive control, the colonies of these three mutant strains were relatively circular in shape. In contrast, Δ*opaR* (as a known hyper swarmer) and Δ*qrr1,3,4,5* mutants showed swarming behaviors (Figure 17). Both mutants presented clear protrusion of the swarming cells from the colonies (Figure 17).

A flowery-like colony morphology of Δ*qrr1,3,4,5* strain was similar to the swarming phenotype appeared in the positive control (Figure 17). While the deletion of other tested *qrrs* showed defect in swarming, wild type swarming was restored with the presence of wild type *qrr2* (Figure 17).

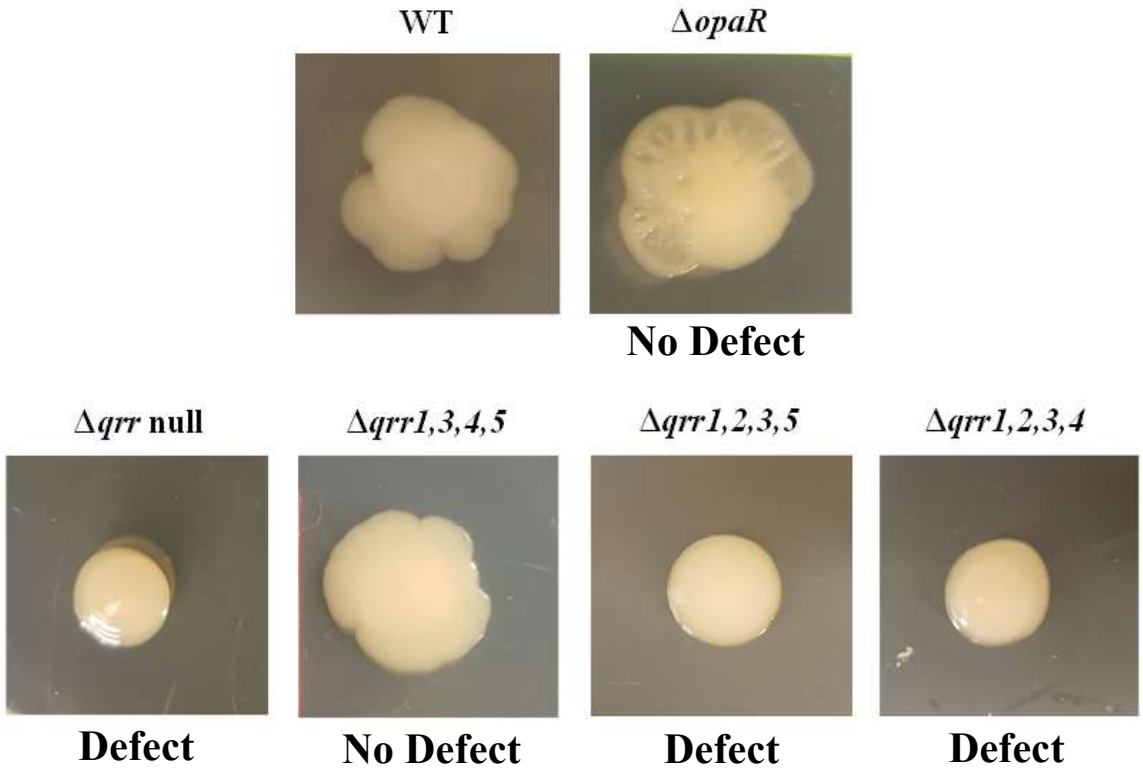

Figure 17 Swarming motility. The phenotypes of the mutants were compared to that of wild type and Δ*opaR*, a hyper swarmer. The Δ*qrr1,3,4,5* mutant swarmed with similar swarming expression relative to wild type. The Δ*qrr* null, Δ*qrr1,2,3,5* and Δ*qrr1,2,3,4* mutants showed defect in swarming.

3.5 Predicted Interactions Between the 5' UTR of *opaR* and *aphA* With Qrrs

Qrrs interact with the mRNAs anti-antisense by base-pairing with the target's 5' untranslated region (UTR). Computational analyses were performed to study the interactions of *V. parahaemolyticus qrrs1-5* with *opaR* and *aphA* mRNA. The 5' UTR of the mRNA targets were acquired from the transcriptional start site (31, 65) to the translational start site of the genes. The lengths of the 5' UTR of *opaR* and *aphA* are 78 and 203 bp, respectively. Figure 18 shows multiple RNA hybridization regions of

qrrs1-5 and the target, *opaR*. Figure 19 also presents multiple base-pairing regions from the interaction of *qrrs1*-5 and the target, *aphA*.

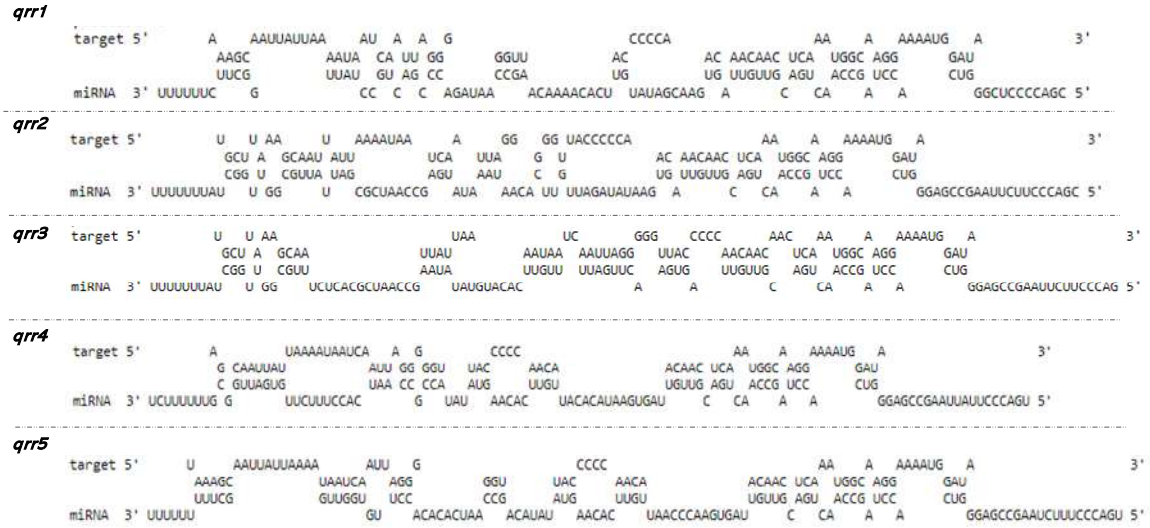

Figure 18 Predicted RNA-RNA interaction analysis of the target: 5' UTR of *opaR* and the miRNA: *qrrs1-5*.

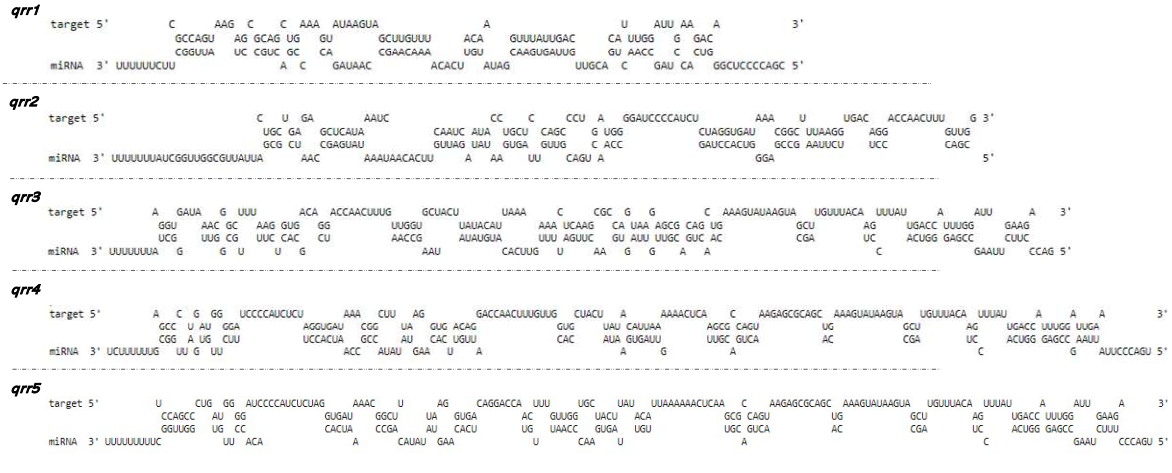

Figure 19 Predicted RNA hybridization analyses of the miRNA: *qrrs1-5* and the target: 5' UTR of *aphA*.

3.6 Predicted Structure of Qrrs1-5 with Base-pairing Regions in Stem Loops

Vibrio harveyi is a very closely related species to *V. parahaemolyticus*. From the study of the Qrrs in *V. harveyi*, it is known all Qrrs are folded into four stem loops (SL). Each of these loops were determined to function in protection, interaction, or termination of their target transcripts.

In this study, the base-pairing regions of the five *V. parahaemolyticus qrrs* with the 5' UTR of *opaR* and *aphA* (Figures 18, 19) were located within the predicted structures. As described in the reference (48), SLs of all Qrrs are in the order of SL1-4 from the 5'end.

In Figures 20-24, predicted RNA-hybridizing regions of the five *V. parahaemolyticus* Qrrs with the 5' UTR of *opaR* are highlighted in red. The predicted base-pairing regions of Qrrs1-5 with the 5' UTR of *aphA* are highlighted in yellow. The base-pairing regions were located in stem loops (SL). The SL1 and SL2 were especially noted, as these loops were determined to interact with target mRNAs previously for sRNA from other *Vibrio* species (48).

The base-pairing interaction of Qrr1 with *opaR* and *aphA* mRNAs were located within SL2 and partial binding in SL4 (Figure 20), and Qrr2 pairing regions with *opaR* mRNA were within SL2 and SL4 (Figure 21). However, the base- pairing regions of Qrr2 with *aphA* mRNA were found in SL1 and SL3. The Qrr2 pairing regions located in SL1, SL2 and SL3 are of note as these could possibly be involved in the Qrr2 unique regulation of OpaR and AphA. The RNA-hybridizing regions of Qrr3 with the 5' UTR of *opaR* were found only in SL2 and SL3, and with the 5' UTR of *aphA* were

located within all four SLs, with partial binding in SL1 (Figure 22). The base-pairing regions of Qrr4 with *aphA* mRNA were located within all four SLs (Figure 23), however, SL2 was the only loop showing the pairing interaction with *opaR*. In Qrr5, the RNA-hybridizing regions with *opaR* were observed in SL2 and SL4, and *aphA* involved all four SLs, with partial binding in SL1 (Figure 24).

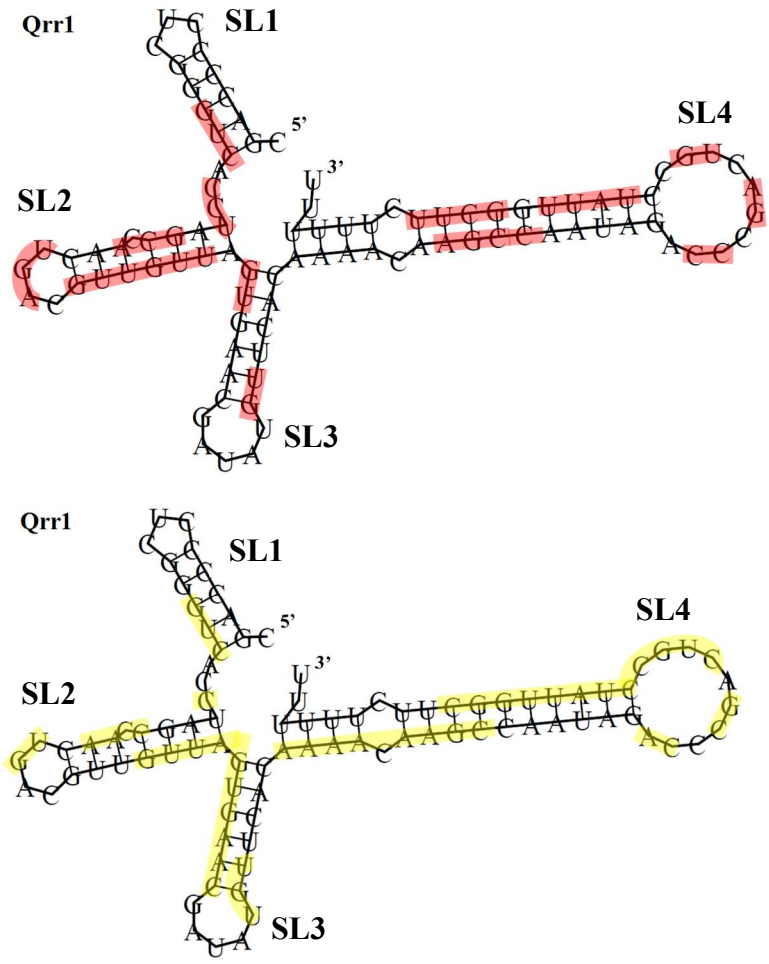

Figure 20 The predicted folding of Qrr1, presented with four stem loops. The top structure shows the Qrr1 base pairing regions with the 5' UTR of *opaR*, highlighted in red. The bottom structure shows the interacting regions with the 5' UTR of *aphA*, highlighted in yellow. Qrr1 interacting regions with both targets are located within SL2 and partial SL4.

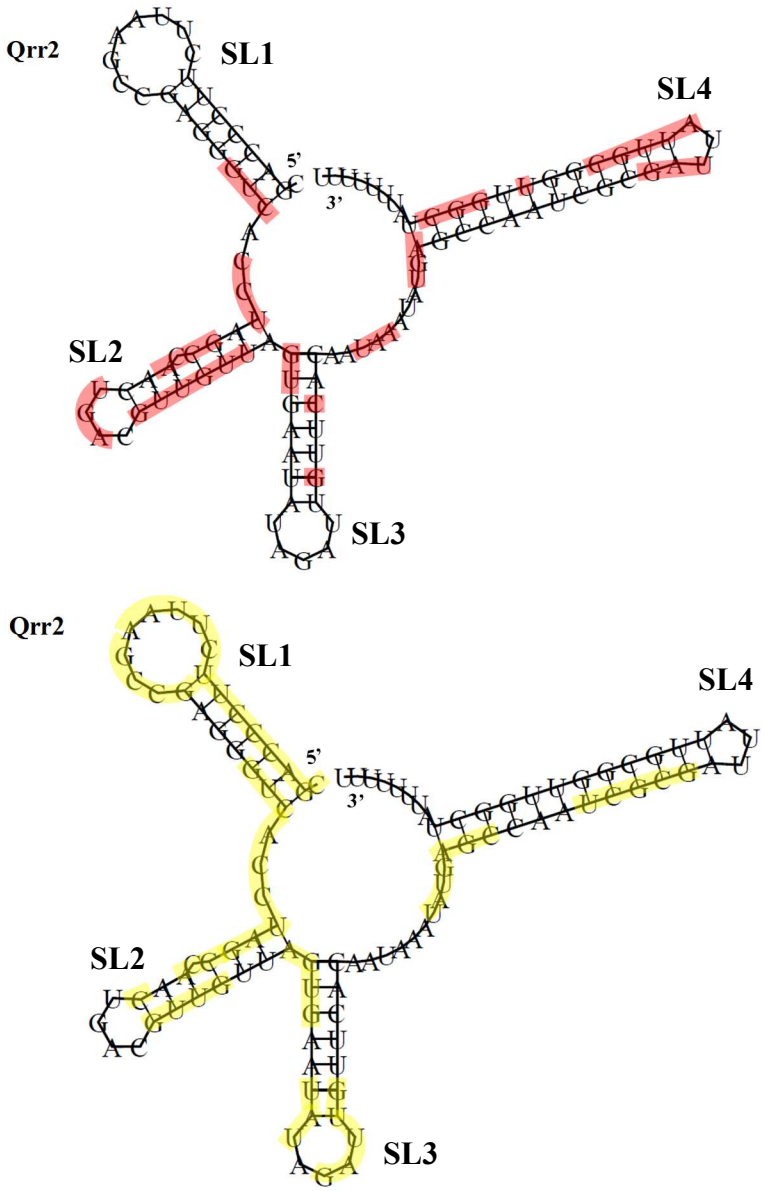

Figure 21 The predicted structure of Qrr2 folded into four loops. The top Qrr2 highlighted in red indicate the interacting regions with the 5' UTR of *opaR*. The highlighted regions in yellow at the bottom Qrr2 indicate the pairing regions with the 5' UTR of *aphA.* Qrr2 base-pairing regions with *opaR* are located within SL2 and SL4, and the pairing regions with *aphA* are located within SL1 and SL3.

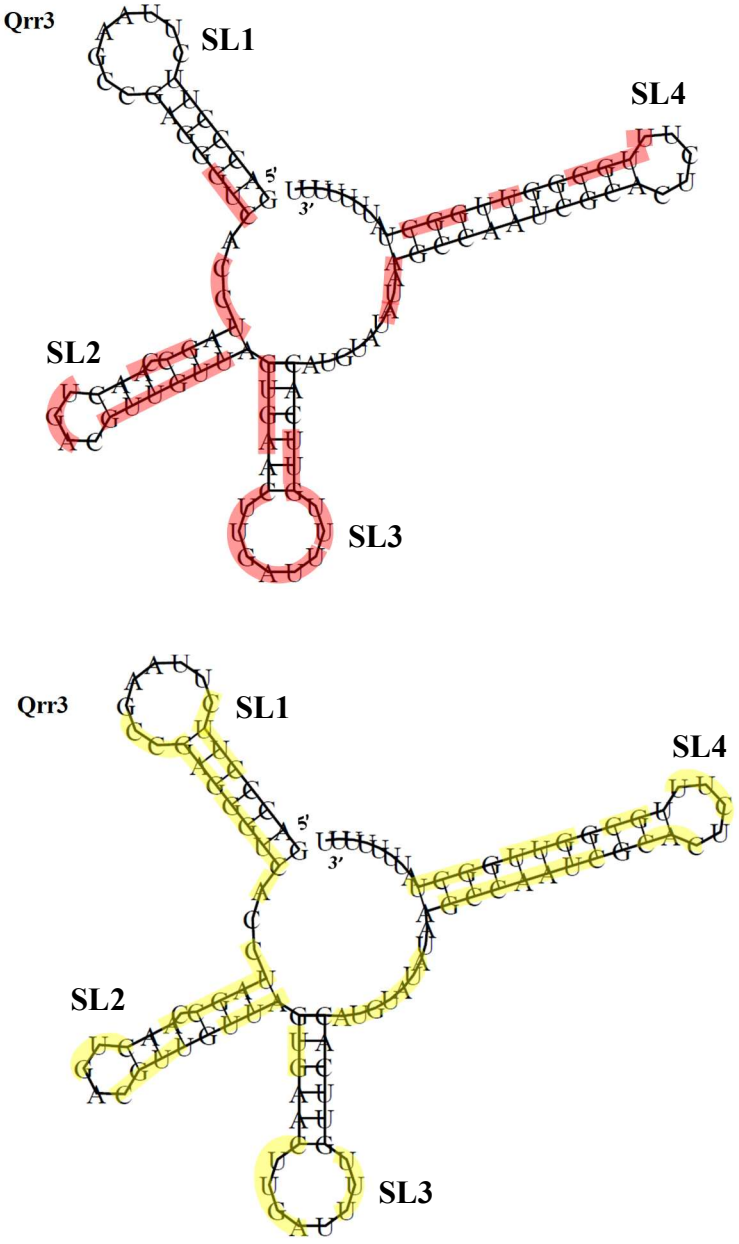

Figure 22 The predicted structure of Qrr3 with four stem loops (SL). The top Qrr3 shows the base pairing interactions with the 5' UTR of *opaR*, in red highlight. The bottom Qrr3 shows the interactions with the 5' UTR of *aphA*, in yellow highlight. Qrr3 interacts with *opaR* mRNA at SL2 and SL3, Qrr3 binds with *aphA* mRNA at SL2, SL3, SL4 and partial SL1.

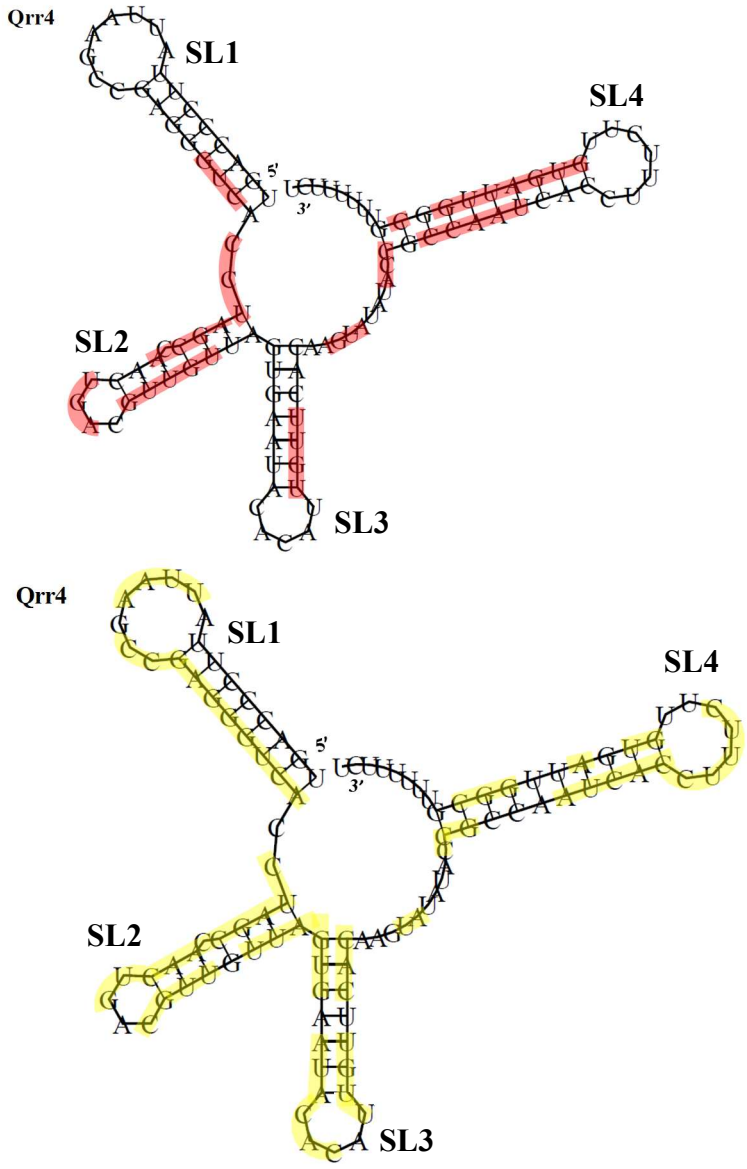

Figure 23 The predicted structure of Qrr4 with four stem loops. The top structure highlighted in red represents the base pairing regions with the 5' UTR of *opaR*. The bottom structure highlighted in yellow represents the interacting regions with the 5' UTR of *aphA*. The Qrr4 base-pairing region with *opaR* is found in SL2, and the pairing regions with *aphA* are located within SL1, SL2, SL3 and SL4.

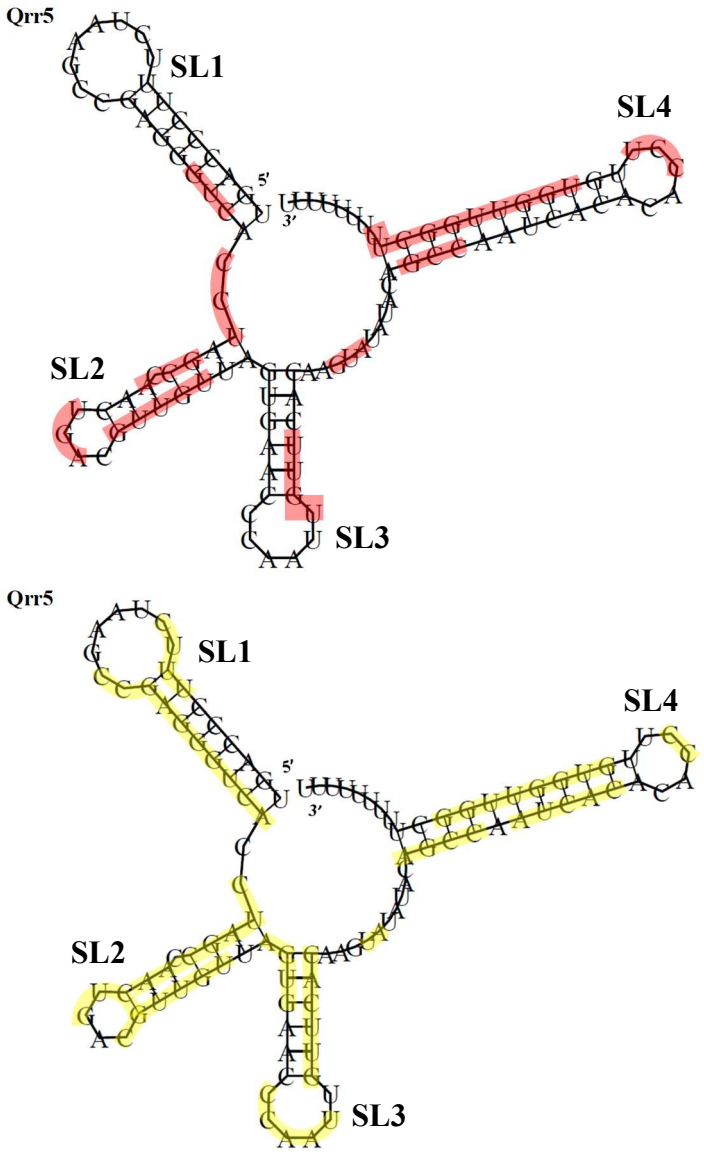

Figure 24 The predicted structure of Qrr5 folded into four stem loops (SL). The top Qrr5 highlights in red the pairing-regions with the 5' UTR of *opaR*. The bottom Qrr5 in yellow highlights the pairing regions with the 5' UTR of *aphA*. The interacting regions with *opaR* are located within SL2 and SL4. Base-pairing regions with *aphA* are located within SL2, SL3 and SL4 and partial SL1.

Table 2 Summarization of the *V. parahaemolyticus* Qrrs1-5 stem loops interaction with the 5' UTR of *opaR* and *aphA*.

Qrrs	Stem Loop (SL)	Interaction with the 5' UTR of *opaR*	Interaction with the 5' UTR of *aphA*
Qrr1	**SL1**	No Interaction	No Interaction
	SL2	Yes	Yes
	SL3	No Interaction	No Interaction
	SL4	Partial Interaction	Partial Interaction
Qrr2	**SL1**	No Interaction	Yes
	SL2	Yes	No Interaction
	SL3	No Interaction	Yes
	SL4	Yes	No Interaction
Qrr3	**SL1**	No Interaction	Partial Interaction
	SL2	Yes	Yes
	SL3	Yes	Yes
	SL4	No Interaction	Yes
Qrr4	**SL1**	No Interaction	Yes
	SL2	Yes	Yes
	SL3	No Interaction	Yes
	SL4	No Interaction	Yes
Qrr5	**SL1**	No Interaction	Partial Interaction
	SL2	Yes	Yes
	SL3	No Interaction	Yes
	SL4	Yes	Yes

3.7 The Alignment Shows the *qrrs1-5* of *V. parahaemolyticus* are Conserved

The Qrrs play important roles in regulating the mRNA through the anti-antisense base-pairing mechanism. The Qrrs sequences are important in the interaction of the target transcripts. The alignment of *qrrs1-5* is shown in Figure 25. The * sign at the bottom of the alignment indicate the conserved sequences among all five *qrrs*. The alignment shows that all *qrrs1-5* are conserved in *V. parahaemolyticus*, however *qrr2, qrr3, qrr4* and *qrr5* show the highest homology. Among these, *qrr1* is shorter and shows less conservation.

```
qrr1            CGACCCCTC---------GGGTCACCTAGCCAACTGACGTTGTTAGTGAA
qrr2            CGACCCTTCTTAAGCCGAGGGTCACCTAGCCAACTGACGTTGTTAGTGAA
qrr3            -GACCCTTCTTAAGCCGAGGGTCACCTAGCCAACTGACGTTGTTAGTGAA
qrr4            TGACCCTTATTAAGCCGAGGGTCACCTAGCCAACTGACGTTGTTAGTGAA
qrr5            TGACCCTTTCTAAGCCGAGGGTCACCTAGCCAACTGACGTTGTTAGTGAA
                 ***** *          ********************************

qrr1            CG--A-TATGTTCACAAA----ACA-AGCCAATAGACCCGACTGCCTATT
qrr2            TAT-AGATTGTTCACAATAAATATG-AGCCAATCG-CGATTATTGCGGTT
qrr3            CTTGATTTTGTTCACATG-TATATA-AGCCAATCG-CACTCTTTGCGGTT
qrr4            TAC-ACATTGTTCACAAG-TATATACCGCCAATCA-CCTTTCTTGTGATT
qrr5            CCC-A-ATTGTTCACAAG-TATATACAGCCAATCA-CACACCTTGTGGTT
                    *   ********      *    ******   *     *     **

qrr1            GGCTTCTTTTTT
qrr2            GGCTATTTTTTT
qrr3            GGCTATTTTTTT
qrr4            GGCGTTTTTTCT
qrr5            GGCTTTTTTTTT
                ***   **** *
```

Figure 25 Constructed alignment of five *qrrs1-5* in *V. parahaemolyticus.* The sign, * indicates conserved sequences across all *qrrs.* The alignment shows that all *V. parahaemolyticus qrrs1-5* are conserved. Among these five *qrrs, qrr1* is the least similar with more polymorphic base pairs and a shorter sequence. Yellow indicates polymorphic sites unique to *qrr2*.

Chapter 4

DISCUSSION

4.1 Restoration of Wild Type CPS Expression, Swimming and Swarming Motility In Δ*qrr1,3,4,5* mutant Strain

In the quorum sensing pathway of *V. parahaemolyticus*, at LCD, five regulatory sRNAs known as *qrrs1-5* are transcribed. These *qrrs1-5* post-transcriptionally stabilize *aphA* mRNA and destabilize *opaR* mRNA. At HCD, the lack of *qrrs1-5* ultimately results in the stabilization of *opaR*, and destabilization of *aphA* (31, 34, 43, 56, 65). These two master quorum sensing regulators play roles in the expression of three phenotypes of cells we analyzed in the study. AphA is known to activate the swimming and swarming motility of the cell. OpaR, a homolog of LuxR, is known to activate CPS of the cell (2, 31).

The CPS, swimming and swarming assays presented various phenotypic results among the tested mutant strains. In the CPS assay, Δ*qrr1,2,3,5* mutant showed a translucent, non-CPS producing colony morphology very similar to that of Δ*opaR,* the negative control. When compared to the positive control, Δ*qrr1,2,3,4* and Δ*qrr* null mutants presented very small colonies with a rough surface. Further work is needed to determine whether CPS is formed in these two mutants. However, we observed Δ*qrr1,3,4,5* mutant expressed a very similar CPS expression relative to wild type.

In the analysis of swimming assay with wild type, Δ*opaR*, Δ*qrr* null and Δ*qrr1,3,4,5* strains, we observed only Δ*qrr1,3,4,5* mutant restored wild type swimming motility. The statistical analysis showed Δ*opaR* mutant had a significantly higher mean swimming diameter relative to wild type. In contrast, Δ*qrr* null had a significantly lower average diameter of swimming cells when compared to wild type. However, there was no significant difference of the mean diameter between wild type and Δ*qrr1,3,4,5* mutant strain.

In the swarming assay, the same strains used in CPS assay were used, and Δ*opaR* and Δ*qrr1,3,4,5* mutants expressed swarming. Amongst the tested *qrrs* mutants, only the Δ*qrr1,3,4,5* mutant restored wild type swarming motility. Meanwhile, the Δ*qrr* null, Δ*qrr1,2,3,5,* Δ*qrr1,2,3,4* mutants showed defect in swarming. When compared to wild type, these mutants presented relatively circular, non-protruding colony morphologies.

Overall observations show the deletion of five *qrrs* resulted in differences in expression of CPS and defective swimming and swarming behaviors compared to wild type. On the other hand, among the tested *qrrs* mutants, we observed the presence of *qrr2* alone could restored wild type CPS swimming and swarming expression. With this unique observation of Δ*qrr1,3,4,5* phenotypes, we decided to focus on *V. parhaemolyticus* Qrr2 in this study.

4.2 Hypothesizing the Base-pairing Interactions of Qrr2 SL2 regulates OpaR, and SL1 and SL3 Regulates AphA

Qrrs interact with the 5'untranslated regions of the target mRNAs by base-pairing anti-antisense (36, 39). Previous studies of quorum sensing in *V. harveyi* determined all Qrrs1-5 are folded into four stem loops (SL), and each loop has a specific function. The first two, SL1 and SL2 interact with the target transcripts by base-pairing to them (48). The loops are in the order of SL1-SL4 from 5'end (48). The SL1 and SL2 perform core-interaction with genes through base-pairings, and SL3 stabilize RNAs or assist in the interaction (48). Our computational analyses predicted multiple base-pair interactions of *V. parahaemolyticus qrrs1-5* with the 5' UTR of *opaR,* and *aphA*. A lot of the interacting regions were located within the folded loops (Figures 20-24) and we focused in studying Qrr2. The predicted regions of Qrr2 base-pair with the 5' UTR of *opaR* were located within SL2 and SL4. The predicted regions of Qrr2 interacting with the 5' UTR of *aphA* were observed within SL1 and SL3 (Figure 21). We hypothesized the observed restoration of wild type CPS expression in Δ*qrr1,3,4,5* mutant is possibly associated with the Qrr2 base-pairing interaction with *opaR* in SL2. In addition, we also hypothesized the restoration of wild type swimming and swarming motility is associated with the Qrr2 interaction with *aphA* in SL1 and SL3. These preliminary analysis of Qrr2 suggests further work is needed in order to understand the Qrr2 regulation of OpaR and AphA, and to identify the difference between Qrr2 and other Qrrs.

4.3 Future Direction

This study showed among the tested *Vibrio parahaemolyticus qrrs* mutants, the presence of *qrr2* alone could restore wild type CPS production, swimming, and swarming motility. From the phenotypic and computational analysis, we hypothesized in Qrr2, SL2 is associated with regulation of OpaR, and SL1 and SL3 are associated with the regulation of AphA.

In the future, the analysis of the CPS, swimming, and swarming expression with the constructed mutants Δ*qrr2,3,4,5* and Δ*qrr1,2,4,5* need to be completed. The data observed from these assays will help determine the role of each individual Qrrs1-5 in the quorum sensing pathway of *V. parahaemolyticus*.

In addition, computational analysis of Qrr1, Qrr3, Qrr4, Qrr5 and their roles in regulating AphA and OpaR are yet to be investigated. Further computational analyses need to be completed in order to fully understand how the stems loops of the five *V. parahaemolyticus* Qrrs regulate *opaR* and *aphA* mRNA.

Finally, our studies are the first to show unique interactions and phenotypes of *qrr* mutants in *V. parahaemolyticus* and they show that although the component of the quorum sensing pathway may be similar between species, their role and mechanism of regulation can be very different.

REFERENCES

1.Atsumi T, McCarter L and Imae Y. Polar and lateral flagellar motors of marine Vibrio are driven by different ion-motive forces. *Nature* 355: 182-184, 1992.

2.Ball AS, Chaparian RR and van Kessel JC. Quorum Sensing Gene Regulation by LuxR/HapR Master Regulators in Vibrios. *J Bacteriol* 199: 2017.

3.Ball AS and van Kessel JC. The master quorum-sensing regulators LuxR/HapR directly interact with the alpha subunit of RNA polymerase to drive transcription activation in Vibrio harveyi and Vibrio cholerae. *Mol Microbiol* 111: 1317-1334, 2019.

4.Bardill JP and Hammer BK. Non-coding sRNAs regulate virulence in the bacterial pathogen Vibrio cholerae. *RNA Biol* 9: 392-401, 2012.

5.Bockemühl J, Roch K, Wohlers B, Aleksic V, Aleksic S, Wokatsch R. Seasonal distribution of facultatively enteropathogenic vibrios (Vibrio cholerae, Vibrio mimicus, Vibrio parahaemolyticus) in the freshwater of the Elbe River at Hamburg. *J Appl Bacteriol* 60: 435-442, 1986.

6.Bonnin-Jusserand M, Copin S, Le Bris C, Brauge T, Gay M, Brisabois A, Grard T, Midelet-Bourdin G. Vibrio species involved in seafood-borne outbreaks (Vibrio cholerae, V. parahaemolyticus and V. vulnificus): Review of microbiological versus recent molecular detection methods in seafood products. *Crit Rev Food Sci Nutr* 59: 597-610, 2019.

7.Case RJ, Labbate M and Kjelleberg S. AHL-driven quorum-sensing circuits: their frequency and function among the Proteobacteria. *ISME J* 2: 345-349, 2008.

8.Daniels NA, MacKinnon L, Bishop R, Altekruse S, Ray B, Hammond RM, Thompson S, Wilson S, Bean NH, Griffin PM, Slutsker L. Vibrio parahaemolyticus infections in the United States, 1973-1998. *J Infect Dis* 181: 1661-1666, 2000.

9.Daniels NA, Ray B, Easton A, Marano N, Kahn E, McShan AL, Del Rosario L, Baldwin T, Kingsley MA, Puhr ND, Wells JG, Angulo FJ. Emergence of a new Vibrio parahaemolyticus serotype in raw oysters: A prevention quandary. *JAMA* 284: 1541-1545, 2000.

10.Enos-Berlage JL, Guvener ZT, Keenan CE, McCarter LL. Genetic determinants of biofilm development of opaque and translucent Vibrio parahaemolyticus. *Mol Microbiol* 55: 1160-1182, 2005.

11.Enos-Berlage JL and McCarter LL. Relation of capsular polysaccharide production and colonial cell organization to colony morphology in Vibrio parahaemolyticus. *J Bacteriol* 182: 5513-5520, 2000.

12.Feng L, Rutherford ST, Papenfort K, Bagert JD, van Kessel JC, Tirrell DA, Wingreen NS, Bassler BL. A qrr noncoding RNA deploys four different regulatory mechanisms to optimize quorum-sensing dynamics. *Cell* 160: 228-240, 2015.

13.Ferreira RB, Antunes LC, Greenberg EP, McCarter LL. Vibrio parahaemolyticus ScrC modulates cyclic dimeric GMP regulation of gene expression relevant to growth on surfaces. *J Bacteriol* 190: 851-860, 2008.

14.Fröhlich KS and Vogel J. Activation of gene expression by small RNA. *Curr Opin Microbiol* 12: 674-682, 2009.

15.Gao H, Zhang L, Osei-Adjei G, Yang W, Zhou D, Huang X, Yang H, Yin Z, Zhang Y. Transcriptional regulation of cpsQ-mfpABC and mfpABC by CalR in Vibrio parahaemolyticus. *Microbiologyopen* 6: 2017.

16.Geske GD, O'Neill JC and Blackwell HE. Expanding dialogues: from natural autoinducers to non-natural analogues that modulate quorum sensing in Gram-negative bacteria. *Chem Soc Rev* 37: 1432-1447, 2008.

17.Gibson DG. Enzymatic assembly of overlapping DNA fragments. *Methods Enzymol* 498: 349-361, 2011.

18.Gibson DG, Young L, Chuang RY, Venter JC, Hutchison CA, Smith HO. Enzymatic assembly of DNA molecules up to several hundred kilobases. *Nat Methods* 6: 343-345, 2009.

19.Güvener ZT and McCarter LL. Multiple regulators control capsular polysaccharide production in Vibrio parahaemolyticus. *J Bacteriol* 185: 5431-5441, 2003.

20.Heckman KL and Pease LR. Gene splicing and mutagenesis by PCR-driven overlap extension. *Nat Protoc* 2: 924-932, 2007.

21.Horton RM, Ho SN, Pullen JK, Hunt HD, Cai Z, Pease LR. Gene splicing by overlap extension. *Methods Enzymol* 217: 270-279, 1993.

22.Hsieh YC, Liang SM, Tsai WL, Chen YH, Liu TY, Liang CM. Study of capsular polysaccharide from Vibrio parahaemolyticus. *Infect Immun* 71: 3329-3336, 2003.

23.Jaques S and McCarter LL. Three new regulators of swarming in Vibrio parahaemolyticus. *J Bacteriol* 188: 2625-2635, 2006.

24.Kalburge SS, Carpenter MR, Rozovsky S, Boyd EF. Quorum Sensing Regulators Are Required for Metabolic Fitness in Vibrio parahaemolyticus. *Infect Immun* 85: 2017.

25.Kearns DB. A field guide to bacterial swarming motility. *Nat Rev Microbiol* 8: 634-644, 2010.

26.Krüger J and Rehmsmeier M. RNAhybrid: microRNA target prediction easy, fast and flexible. *Nucleic Acids Res* 34: W451-454, 2006.

27.Lilley BN and Bassler BL. Regulation of quorum sensing in Vibrio harveyi by LuxO and sigma-54. *Mol Microbiol* 36: 940-954, 2000.

28.Madeira F, Park YM, Lee J, Buso N, Gur T, Madhusoodanan N, Basutkar P, Tivey ARN, Potter SC, Finn RD, Lopez R. The EMBL-EBI search and sequence analysis tools APIs in 2019. *Nucleic Acids Res* 47: W636-W641, 2019.

29.Marx CJ. Development of a broad-host-range sacB-based vector for unmarked allelic exchange. *BMC Res Notes* 1: 1, 2008.

30.Małecka EM, Stróżecka J, Sobańska D, Olejniczak M. Structure of bacterial regulatory RNAs determines their performance in competition for the chaperone protein Hfq. *Biochemistry* 54: 1157-1170, 2015.

31.McCarter LL. OpaR, a homolog of Vibrio harveyi LuxR, controls opacity of Vibrio parahaemolyticus. *J Bacteriol* 180: 3166-3173, 1998.

32.McLaughlin JB, DePaola A, Bopp CA, Martinek KA, Napolilli NP, Allison CG, Murray SL, Thompson EC, Bird MM, Middaugh JP. Outbreak of Vibrio parahaemolyticus gastroenteritis associated with Alaskan oysters. *N Engl J Med* 353: 1463-1470, 2005.

33.Morett E and Buck M. In vivo studies on the interaction of RNA polymerase-sigma 54 with the Klebsiella pneumoniae and Rhizobium meliloti nifH promoters. The role of NifA in the formation of an open promoter complex. *J Mol Biol* 210: 65-77, 1989.

34.Ng WL and Bassler BL. Bacterial quorum-sensing network architectures. *Annu Rev Genet* 43: 197-222, 2009.

35.Notredame C, Higgins DG and Heringa J. T-Coffee: A novel method for fast and accurate multiple sequence alignment. *J Mol Biol* 302: 205-217, 2000.

36.Oliva G, Sahr T and Buchrieser C. Small RNAs, 5' UTR elements and RNA-binding proteins in intracellular bacteria: impact on metabolism and virulence. *FEMS Microbiol Rev* 39: 331-349, 2015.

37.Papenfort K and Bassler BL. Quorum sensing signal-response systems in Gram-negative bacteria. *Nat Rev Microbiol* 14: 576-588, 2016.

38.Philippe N, Alcaraz JP, Coursange E, Geiselmann J, Schneider D. Improvement of pCVD442, a suicide plasmid for gene allele exchange in bacteria. *Plasmid* 51: 246-255, 2004.

39.Pérez-Reytor D, Plaza N, Espejo RT, Navarrete P, Bastías R, Garcia K. Role of Non-coding Regulatory RNA in the Virulence of Human Pathogenic. *Front Microbiol* 7: 2160, 2016.

40.Rahimzadeh M, Sadeghizadeh M, Najafi F, Arab S, Mobasheri H. Impact of heat shock step on bacterial transformation efficiency. *Mol Biol Res Commun* 5: 257-261, 2016.

41.Rehmsmeier M, Steffen P, Hochsmann M, Giegerich R. Fast and effective prediction of microRNA/target duplexes. *RNA* 10: 1507-1517, 2004.

42.Reyrat JM, Pelicic V, Gicquel B, Rappuoli R. Counterselectable markers: untapped tools for bacterial genetics and pathogenesis. *Infect Immun* 66: 4011-4017, 1998.

43.Rutherford ST, van Kessel JC, Shao Y, Bassler BL. AphA and LuxR/HapR reciprocally control quorum sensing in vibrios. *Genes Dev* 25: 397-408, 2011.

44.Sar N, McCarter L, Simon M, Silverman M. Chemotactic control of the two flagellar systems of Vibrio parahaemolyticus. *J Bacteriol* 172: 334-341, 1990.

45.Sawabe T, Ogura Y, Matsumura Y, Feng G, Amin AR, Mino S, Nakagawa S, Kumar R, Fukui Y, Satomi M, Matsushima R, Thompson FL, Gomez-Gil B, Christen R, Maruyama F, Kurokawa K, Hayashi T. Updating the Vibrio clades

defined by multilocus sequence phylogeny: proposal of eight new clades, and the description of Vibrio tritonius sp. nov. *Front Microbiol* 4: 414, 2013.

46.Scallan E, Hoekstra RM, Angulo FJ, Tauxe RV, Widdowson MA, Roy SL, Jones JL, Griffin PM. Foodborne illness acquired in the United States--major pathogens. *Emerg Infect Dis* 17: 7-15, 2011.

47.Shao Y and Bassler BL. Quorum-sensing non-coding small RNAs use unique pairing regions to differentially control mRNA targets. *Mol Microbiol* 83: 599-611, 2012.

48.Shao Y, Feng L, Rutherford ST, Papenfort K, Bassler BL. Functional determinants of the quorum-sensing non-coding RNAs and their roles in target regulation. *EMBO J* 32: 2158-2171, 2013.

49.Shinoda S and Okamoto K. Formation and function of Vibrio parahaemolyticus lateral flagella. *J Bacteriol* 129: 1266-1271, 1977.

50.Silveira AC, Robertson KL, Lin B, Wang Z, Vora GJ, Vasconcelos AT, Thompson FL. Identification of non-coding RNAs in environmental vibrios. *Microbiology* 156: 2452-2458, 2010.

51.Srivastava D and Waters CM. A tangled web: regulatory connections between quorum sensing and cyclic Di-GMP. *J Bacteriol* 194: 4485-4493, 2012.

52.Su YC and Liu C. Vibrio parahaemolyticus: a concern of seafood safety. *Food Microbiol* 24: 549-558, 2007.

53.Terashima H, Kojima S and Homma M. Flagellar motility in bacteria structure and function of flagellar motor. *Int Rev Cell Mol Biol* 270: 39-85, 2008.

54.Thompson FL, Iida T and Swings J. Biodiversity of vibrios. *Microbiol Mol Biol Rev* 68: 403-431, table of contents, 2004.

55.Trimble MJ and McCarter LL. Bis-(3'-5')-cyclic dimeric GMP-linked quorum sensing controls swarming in Vibrio parahaemolyticus. *Proc Natl Acad Sci U S A* 108: 18079-18084, 2011.

56.Tu KC and Bassler BL. Multiple small RNAs act additively to integrate sensory information and control quorum sensing in Vibrio harveyi. *Genes Dev* 21: 221-233, 2007.

57.van Kessel JC, Rutherford ST, Shao Y, Utria AF, Bassler BL. Individual and combined roles of the master regulators AphA and LuxR in control of the Vibrio harveyi quorum-sensing regulon. *J Bacteriol* 195: 436-443, 2013.

58.Van Puyvelde S, Vanderleyden J and De Keersmaecker SC. Experimental approaches to identify small RNAs and their diverse roles in bacteria--what we have learnt in one decade of MicA research. *Microbiologyopen* 4: 699-711, 2015.

59.Wagner EG. Cycling of RNAs on Hfq. *RNA Biol* 10: 619-626, 2013.

60.Wang L, Ling Y, Jiang H, Qiu Y, Qiu J, Chen H, Yang R, Zhou D. AphA is required for biofilm formation, motility, and virulence in pandemic Vibrio parahaemolyticus. *Int J Food Microbiol* 160: 245-251, 2013.

61.Waters LS and Storz G. Regulatory RNAs in bacteria. *Cell* 136: 615-628, 2009.

62.West PA. The human pathogenic vibrios--a public health update with environmental perspectives. *Epidemiol Infect* 103: 1-34, 1989.

63.Whitaker WB, Richards GP and Boyd EF. Loss of sigma factor RpoN increases intestinal colonization of Vibrio parahaemolyticus in an adult mouse model. *Infect Immun* 82: 544-556, 2014.

64.Yang C, Zhang X, Fan H, Li Y, Hu Q, Yang R, Cui Y. Genetic diversity, virulence factors and farm-to-table spread pattern of Vibrio parahaemolyticus food-associated isolates. *Food Microbiol* 84: 103270, 2019.

65.Zhang Y, Qiu Y, Tan Y, Guo Z, Yang R, Zhou D. Transcriptional regulation of opaR, qrr2-4 and aphA by the master quorum-sensing regulator OpaR in Vibrio parahaemolyticus. *PLoS One* 7: e34622, 2012.

66. http://rna.tbi.univie.ac.at/cgi-bin/RNAWebSuite/RNAfold.cgi

67. https://www.cdc.gov/vibrio/.

Appendix A

PRIMERS USED IN THE STUDY

Table 3 Lists of primers used in the study. The restriction enzymes sequences are show in blue.

Primers	Sequence (5'-3')	Product size (BP)	Annealing Temperature (°C)
Gibson Assembly *qrr1* A	CATGCGATATCGAGCTGAATTGCGTTGTTGACCG	1197	57.5
Gibson Assembly *qrr1* D	ATTCCCGGGAGAGCTGATATGCCGGAAGTCTCG		
Gibson Assembly *qrr1* Flanking Forward	TTCATCGAGGAACAACGTGC	1873	57.5
Gibson Assembly *qrr1* Flanking Reverse	GCCGGGCAATTATGAGCTAG		
SOE *qrr2* A	TCTAGAAGAGACGGGTTAATACGACGA	1068	55
SOE *qrr2* D	GAGCTCACCGCGCTCAACAACTAATG		
SOE *qrr2* Flanking Forward	CGCTAAGGTTGCAATGCTCG	1237	62
SOE *qrr2* Flanking Reverse	TTGATGGCGCTACGATTGGT		
SOE *qrr3* A	CACGCATGCATTGCTCAAGTGGTGGCTTT	1250	54
SOE *qrr3* D	CACGAGCTCGCCATTATTACCTCCGCAAA		
SOE *qrr3* Flanking Forward	GCAAAATGACACTGCCAGAA	1887	55.4
SOE *qrr3* Flanking Reverse	GTTGCTTTATGCACCGGAAT		
SOE *qrr4* A	CATGCGATATCGAGCTTGCGCAAGGTTGTCGTAG	1127	57.3
SOE *qrr4* D	ATTCCCGGGAGAGCTATTACCTTGGGGCAACATGC		
Gibson Assembly *qrr5* A	CATGCGATATCGAGCTTTCAAGTTATGAATAGCGATG	1293	52.4
Gibson Assembly *qrr5* D	ATTCCCGGGAGAGCTTTTCTTGGCTTCAACACG		

Appendix B

SUMMARIZATION OF PHENOTYPIC ANALYSIS OF *VIBRIO PARAHAEMOLYTICUS*

Table 4 Characteristics of the capsule polysaccharide productions, swimming and swarming motilities observed in tested strains.

STRAINS	CAPSULE POLYSACCHARIDE (CPS)	SWIM	SWARM
WT	+	+	+
Δ*opaR*	- (smooth and translucent colony with no CPS production)	+ (Hyper swimmer)	+
Δ*qrr* null	+ (Smaller colony size with a rough surface)	-	-
Δ*qrr2,3,4,5*	Data not obtained	Data not obtained	Data not obtained
Δ*qrr1,3,4,5*	+ **(Restored the wild type phenotype of the CPS production)**	+	+
Δ*qrr1,2,4,5*	Data not obtained	Data not obtained	Data not obtained
Δ*qrr1,2,3,5*	- (Translucent colony with no expression of CPS)	Data not obtained	-
Δ*qrr1,2,3,4*	+ (A very similar colony morphology as in Δ*qrr* null Rough surface with a smaller colony)	Data not obtained	-